OPT3 plays a central role in both copper and iron homeostasis and signaling due to its ability to deliver copper as well as iron to the phloem in *Arabidopsis*

Ju-Chen Chia[1], Jiapei Yan[1], Maryam Rahmati Ishka[1], Marta Marie Faulkner[1], Rong Huang[3], Louisa Smieska[3], Arthur Woll[3], Ryan Tappero[4], Andrew Kiss[4], Chen Jiao[5], Zhangjun Fei[5,6], Miguel Piñeros[2,5,6], Leon V. Kochian[6]†, Elsbeth Walker[7], Olena K. Vatamaniuk[1,2*]

[1]Crop and Soil Sciences Section, School of Integrative Plant Science, Cornell University, NY, USA

[2]Plant Biology Section, School of Integrative Plant Science, Cornell University, NY, USA

[3]Cornell High Energy Synchrotron Source (CHESS), Cornell University, NY, USA

[4]National Light Source II, Brookhaven National Laboratory, USA

[5]Boyce Thompson Institute for Plant Research, Ithaca, NY, USA

[6]Robert W. Holley Center for Agriculture and Health, USDA-ARS, NY, USA

[7]University of Massachusetts, MA, USA

†Current address: Global Institute for Food Security, University of Saskatchewan, Saskatoon, Canada.

*Corresponding Author:

Olena K. Vatamaniuk

Email: okv2@cornell.edu

Short title:

AtOPT3 mediates iron - copper crosstalk

Abstract

Copper and iron are micronutrients but are toxic when they accumulate in cells in excess. Crosstalk between copper and iron homeostasis in *Arabidopsis thaliana* has been documented and includes iron accumulation under copper deficiency and *vice versa*. However, molecular components of this crosstalk are not well understood. Iron concentration in the phloem has been suggested to act systemically, negatively regulating iron uptake to the root. Consistently, systemic iron signaling is disrupted in *A. thaliana* mutants lacking the phloem companion cell-localized iron transporter, AtOPT3, and *opt3* mutants hyperaccumulate iron. Here, we report that in addition to iron, AtOPT3 transports copper and mediates copper loading to the phloem for delivery from sources to sinks. As a result of this function, the *opt3-3* mutant accumulates less copper in the phloem, roots, developing leaves and embryos compared to wild type, is sensitive to copper deficiency, and mounts transcriptional copper deficiency response. Because copper deficiency has been shown to stimulate iron accumulation, we propose that reduced copper concentration in the phloem of the *opt3-3* mutant and its constitutive copper deficiency contribute to iron overaccumulation in its tissues. Our data assign new transport capabilities to AtOPT3 and increase understanding of copper - iron interactions and signaling.

Introduction

Iron and copper are essential elements, required in trace amounts to complete the life cycle of all organisms, including plants and humans. However, these elements are toxic to cells if they accumulate in ionic form (Broadley et al., 2012; Ravet and Pilon, 2013). The essential and yet toxic nature of iron and copper is attributed to the ease with which they accept and donate electrons (Broadley et al., 2012; Ravet and Pilon, 2013). This ability has been capitalized by nature for vital physiological processes, including photosynthesis, respiration and scavenging of reactive oxygen species. In addition to these processes, copper is involved in cell wall lignification and reproduction (Epstein and Bloom, 2005; Broadley et al., 2012; Chen et al., 2020; Rahmati Ishka and Vatamaniuk, 2020; Sheng et al., 2021). Recent studies implicate copper in light-dependent seed germination (Jiang et al., 2020), shaping the shoot architecture, transition to flowering, stigmatic papillae development and senescence (Rahmati Ishka and Vatamaniuk, 2020; Sheng et al., 2021). Mounting evidence from studies in animal species also implicates copper in cell signaling through its untraditional role as a modulator of MAPK signaling and mTOR-dependent autophagic kinase signaling (Turski and Thiele, 2009; Turski et al., 2012; Chang, 2015; Tsang et al., 2020). In plants, copper participates in hormone signaling and accumulation (Rodríguez et al., 1999; Wu et al., 2012; Yan et al., 2017; Schott-Verdugo et al., 2019). Iron is also involved in nitrate and sulfate assimilation and chlorophyll synthesis, and ethylene and jasmonic acid accumulation (Broadley et al., 2012; Li and Lan, 2017; Cui et al., 2018).

Copper and iron uptake by plant roots, internal transport and storage are rigorously regulated at transcriptional and posttranscriptional levels in response to the availability of these elements in a local environment and the demands of the developing shoot (Burkhead et al., 2009; Ravet and Pilon, 2013; Kobayashi, 2019; Pottier et al., 2019; Spielmann and Vert, 2020). To maintain copper homeostasis, plants regulate cellular copper uptake and economize on copper by recycling it during deficiency from non-essential to essential copper enzymes (Burkhead et al., 2009; Ravet et al., 2011; Shahbaz et al., 2015). In *A. thaliana*, both processes are controlled by a conserved transcription factor, SPL7 (**S**quamosa **P**romoter Binding Protein–**l**ike7 (Yamasaki et al., 2009; Bernal et al., 2012). In addition to SPL7, a member of the basic helix-loop-helix (bHLH) family, CITF1 (**C**opper Deficiency-**i**nduced **T**ranscription **F**actor 1, *alias* bHLH160) regulates copper uptake into roots, delivery to leaves, flowers and anthers (Yan et al., 2017).

CITF1 acts together with SPL7, and the function of both is required for copper delivery to reproductive organs and fertility (Yan et al., 2017). SPL7-dependent regulon includes Iron (**F**e)/Cu **r**eductase **o**xidases, *FRO4* and *FRO5*, and several copper transporters, including *COPT1*, *COPT2* and, in part, *COPT6*, that are members of the CTR/COPT/SLC31 (**C**opper **T**ransporter/**Cop**per **T**ransporter/**Sol**ute **C**arrier **31**) family (Yamasaki et al., 2009; Bernal et al., 2012; Jung et al., 2012; Gayomba et al., 2013; Jain et al., 2014; Araki et al., 2018; Alexander et al., 2019). *FRO4/5* and *COPT2* are also downstream targets of CITF1 (Yan et al., 2017). Altered expression of SPL7- and CITF1-regulated genes and the increased expression of *CITF1* constitute a signature of copper deficiency response.

Regulation of iron homeostasis in *A. thaliana* involves a hierarchy of transcription factors from the bHLH family (Jeong et al., 2017; Kim et al., 2019). Specifically, a member of the IVb subgroup of the bHLH family, URI (Upstream Regulator of IRT1, bHLH121), acts upstream as an iron-dependent switch (Kim et al., 2019; Gao et al., 2020). It heterodimerizes with a subgroup IVc bHLH members to regulate the expression of the master regulator of iron homeostasis FIT (**F**ER-like iron deficiency-induced **t**ranscription factor, alias bHLH29) (Kim et al., 2019; Gao et al., 2020). FIT forms heterodimers with the Ib subgroup of bHLH transcription factors to regulate expression of multiple genes in *A. thaliana* roots, among which are some components of the iron uptake system, *IRT1* (**I**ron-**R**egulated **T**ransporter **1**), *FRO2* and *AHA2* (Plasma Membrane Proton ATPase) (reviewed in (Jeong et al., 2017; Schwarz and Bauer, 2020). The upregulated expression of *Ib bHLH* genes, *FIT*, *AHA2*, *FRO2* and *IRT1*, and the newly discovered *IMA/FEP* is a hallmark of root iron-deficiency response (Jeong et al., 2017; Grillet et al., 2018; Hirayama et al., 2018; Schwarz and Bauer, 2020). Expression of these and other iron-responsive genes is regulated *via* local and systemic iron status signaling (Gayomba et al., 2015; Jeong et al., 2017; Grillet et al., 2018; Hirayama et al., 2018; Schwarz and Bauer, 2020).

Several mutants with the disrupted shoot-to-root iron deficiency signaling have been identified in *A. thaliana* and other plant species all showing constitutive activation of iron-acquisition genes even when grown under iron-sufficient conditions ((Kumar et al., 2017) and reviewed in (Gayomba et al., 2015). Of these, a member of the OPT (**O**ligo **P**eptide **T**ransporter) clade of the OPT transporter family, *A. thaliana* OPT3, is considered as a key player in systemic signaling of iron deficiency (Stacey et al., 2002; Stacey et al., 2008; Mendoza-Cózatl et al., 2014; Zhai et al., 2014). While the *opt3-1* knockout allele is embryo lethal, the *opt3-2* and *opt3-3*

alleles that possess residual levels of *OPT3* expression, hyperaccumulate iron in roots and leaves but cannot turn off the expression of *AHA2*, *IRT1* and *FRO2* and other iron deficiency-responsive genes (Stacey et al., 2002; Stacey et al., 2008; Mendoza-Cózatl et al., 2014; Zhai et al., 2014). AtOPT3 transports iron ions in *Xenopus laevis* oocytes and *Saccharomyces cerevisiae*, localizes to companion cells of the phloem, mediates iron loading to the phloem, and facilitates iron delivery from sources (mature leaves) to sinks (roots and seeds) (Zhai et al., 2014). Based on these findings it is suggested that by loading iron into the phloem in leaves, OPT3 communicates iron sufficiency status to the root. Consistent with this suggestion, the loss of the iron transport function in the *opt3-3* mutant and the decreased iron accumulation in its phloem sap not only leads to a decreased iron accumulation in seeds but also is perceived as the iron deficiency signal by the root (Zhai et al., 2014). Local sensing of high iron status in the shoot seems not to be disrupted in the *opt3* mutant, as evidenced by the increased expression of genes encoding iron-storage proteins *FER3* and *FER4* (Khan et al., 2018).

It is noteworthy that the fluctuations of cellular iron concentrations alter the ratio of other transition elements and thus, have a profound effect on the metal composition of the cell (Baxter et al., 2008). In this regard, crosstalk between iron and copper is now well documented. The hallmark of this crosstalk is the overaccumulation of iron under copper deficiency and overaccumulation of copper under iron deficiency (Bernal et al., 2012; Waters and Armbrust, 2013; Kastoori Ramamurthy et al., 2018; Kroh and Pilon, 2020; Rai et al., 2021; Sheng et al., 2021). Consistent with the increased copper uptake under iron deficiency, iron deficiency acts oppositely from copper deficiency on the expression of copper-deficiency-regulated genes (Waters et al., 2012; Waters et al., 2014; Yan et al., 2017). High iron can also reduce copper accumulation in *A. thaliana* and animal systems (Klevay, 2001; Waters and Armbrust, 2013; Ha et al., 2016). Together, these studies suggest that altered copper or iron accumulation under iron or copper deficiency, or under iron oversupply could disturb the signaling of copper and/or iron status of the shoot transmitted to the root.

Here we show that in addition to iron, AtOPT3 transports copper in *Xenopus* oocytes and *S. cerevisiae*. Loss of this function in the *opt3-3* mutant results in a decreased copper accumulation in the phloem and reduced copper recirculation from sources (mature leaves) to sinks (roots, young leaves, siliques and developing embryos) compared to wild type. In addition, the *opt3-3* mutant experiences copper deficiency as evidenced by low copper accumulation in

roots and young leaves, and increased expression of copper deficiency marker genes. These defects are rescued by copper application. Considering that copper deficiency leads to iron over accumulation in roots and leaves of *A. thaliana*, our data raise an intriguing possibility that decreased copper accumulation in the phloem, roots and young leaves of the *opt3-3* mutant, and its constitutive copper-deficient status contributes to iron overaccumulation in tissues of the *opt3-3* mutant.

Results

The Spatial Distribution of Iron and Copper but not of Manganese or Zinc is Altered in the Vasculature of the *opt3-3* Mutant.

Our previous studies showed that iron concentration in the phloem sap is significantly lower while in the xylem sap is significantly higher in the *opt3-3* mutant compared to wild type (Zhai et al., 2014). This finding suggested that the distribution of iron in the vascular tissue of the mutant *vs.* wild type might have been altered. To test this hypothesis, we used synchrotron x-ray fluorescence (XRF) microscopy to compare the spatial distribution of iron and other elements in the vasculature of the *opt3-3* mutant (from here on referred to as *opt3*) *vs.* wild type. We first evaluated mineral distribution in mature leaves that serve as sources of nutrients for developing leaves at the vegetative stage (**Figure 1**). Consistent with our past findings (Zhai et al., 2014), the *opt3* mutant accumulated more iron throughout the leaf blade, with the bulk of iron located in minor veins compared to wild type (**Figure 1A**). We also found that in addition to iron, mature leaves of the *opt3* mutant accumulated more copper, manganese and zinc (**Figure 1B** to **D**). The spatial distribution of manganese and zinc was not altered in the *opt3* mutant compared to wild type: manganese was spread throughout the leaf blade with the highest accumulation in basal cells of trichomes, while zinc was also noticeable in the vasculature (**Figure 1C, D**). Copper also hyperaccumulated in the vasculature of the *opt3* mutant, and its distribution pattern in minor veins resembled the distribution of iron (**Figure 1A** and **B**). We then used 2D-XRF in a confocal mode (2D-CXRF) using a specialized x-ray collection optic to obtain a micron-scale resolution enabling analyses of mineral localization in the phloem *vs.* xylem in the *opt3* mutant *vs.* wild type. For the current study, this technique is preferable to traditional XRF methods (both 2D XRF and 3D micro-XRF tomography) because it allows quantitative comparisons of metal distributions among different samples without the need to control or limit the sample thickness or

lateral size (Mantouvalou et al., 2012). Using 2D-CXRF, we found that the localization of iron and copper but not of manganese or zinc was altered in the *opt3* mutant compared to wild type (**Figure 1 E** to **H**). Specifically, while iron was evenly distributed between the xylem and the phloem in the wild type, the bulk of iron was associated with the xylem and xylem parenchyma cells in the *opt3* mutant. (**Figure 1E**). Consistent with our past findings (Zhai et al., 2014), the *opt3* mutant accumulated significantly more iron in the xylem and xylem parenchyma cells than wild type. While copper was mainly associated with the phloem in the wild type, the *opt3* mutant accumulated most of the copper in the xylem area (**Figure 1F**). The loss of OPT3 function led to a significant increase in the concentration of manganese and zinc in both the xylem and the phloem of the mutant compared to wild type, but the spatial distribution of these elements in the vasculature was the same as in the wild type (**Figure 1G, H**). These results suggested that in addition to iron, OPT3 may also mediate copper loading to the phloem. Indeed, we found that the concentration of copper in the phloem was significantly decreased in the *opt3* mutant compared to the wild type (**Figure 2A**). The decreased accumulation of copper in the phloem of the *opt3* mutant *vs.* wild type was independently found by the Walker lab (**Supplemental Fig. S1 online**).

Roots, Young Leaves and Developing Embryos of the *opt3* Mutant Accumulate Less Copper.

Past studies have shown that mutant alleles of *OPT3* over accumulate iron, manganese and zinc in roots and leaves (Stacey et al., 2008; Mendoza-Cózatl et al., 2014; Zhai et al., 2014). Since the 2D-CXRF analysis of mineral distribution in the vasculature has also pointed to the role of OPT3 in copper homeostasis, we refined our past analysis of total internal metal accumulation to include copper. Consistent with past findings, roots and both mature and young leaves of the *opt3* mutant accumulated significantly more iron, manganese and zinc compared to the corresponding organs of wild type (**Supplemental Fig. S2 online**). By contrast, the concentration of copper in the *opt3* mutant was reduced to less than 1/3 of the wild type level (**Figure. 2B**). We also found that the copper concentration was higher in mature leaves (sources) and lower in young leaves (sinks) in the *opt3* mutant *vs.* wild type (**Figure 2B**).

We then analyzed copper and other mineral accumulation and distribution in other source tissues such as silique valves and their sinks, developing embryos and seeds (**Figure 3)**. ICP-MS analysis disclosed that silique valves of the *opt3* mutant hyperaccumulated copper, iron,

manganese and zinc compared to wild type (**Figure 3A**). Using 2D-XRF we found that developing embryos of the mutant accumulated less copper and iron but more manganese and zinc (**Figure 3B**), suggesting that copper and iron delivery from sources to sinks is reduced in the mutant *vs.* wild type. It was noticeable that the 2D-XRF detectable spatial distribution of copper in developing embryos was distinct from iron. Specifically, copper was associated primarily with the developing seed coat, while iron was mostly localized in the embryo vasculature in both wild type and the *opt3* mutant.

We then used high-resolution 2D computed tomography XRF (CT-XRF) to visualize minerals in mature seeds. Similar to embryos, copper was associated mainly with the seed coat and was detected throughout the seed and the vasculature (**Figure 3C**). It is noteworthy that in some areas of the seed coat, copper concentration was lower in the wild type than in the mutant, while the level of copper in the vasculature was lower in the mutant than in the same areas of wild type (**Figure 3C**). This subtle difference in copper distribution in mutant *vs.* wild type seeds translated to the overall similar internal seed copper concentration in both genotypes (**Figure 3D**). As was shown previously, iron was associated with the vascular parenchyma cells in mature wild type seeds (Kim et al., 2006). Iron distribution did not change in the mutant, although iron accumulation in the *opt3* vascular parenchyma cells was significantly lower than in wild type (**Figure 3C**). Consistently, the total internal iron concentration was lower in the *opt3* mutant seeds *vs.* wild type (**Figure 3D**). While the distribution of manganese and zinc did not change in the mutant *vs.* wild type, the *opt3* mutant seeds accumulated significantly more zinc (**Figure. 3C, D**). Together, our data suggested that OPT3 contributes to the phloem-based redistribution of copper from mature leaves to young leaves and from silique valves to developing embryos, and thus, in addition to iron may also transport copper.

OPT3 Mediates Copper Transport in Heterologous Systems.

The ability of OPT3 to transport copper was studied in *Xenopus laevis* oocytes as we have previously shown that in this expression system, OPT3 localizes to the plasma membrane and transports iron and cadmium ions (Zhai et al., 2014). As potential transport substrates, we tested Cu^{2+} (provided as $CuSO_4$) and copper complexed with its established ligand, nicotianamine (Cu-NA) (**Figure 4)**. We found that OPT3 transported both free copper ions as well as the Cu-NA complex (**Figure 4A**). However, it is noteworthy that OPT3-expressing oocytes accumulated 4.2

times more copper when it was provided as a free ion rather than when complexed with nicotianamine (NA). This finding suggested that free copper ions are a preferred OPT3 substrate, at least in this heterologous system.

The ability of OPT3 to transport copper was further validated by functional complementation assays in the *S. cerevisiae*, which lack the capability to synthesize nicotianamine. We used a copper-deficient *S. cerevisiae ctr1Δctr2Δctr3Δ* mutant lacking the high-affinity plasma membrane copper uptake transporters Ctr1p and Ctr3p and the vacuolar membrane copper efflux transporter, Ctr2p (Dancis et al., 1994; Rees et al., 2004). Due to low internal copper, the *ctr1Δctr2Δctr3Δ* mutant cells manifest a respiratory defect because of the altered activity of the copper-dependent cytochrome *c* oxidase complex of the mitochondrial respiratory chain. This defect can be visualized by the failure of the *ctr1Δctr2Δctr3Δ* mutant to grow on non-fermentable carbon sources such as ethanol and glycerol (YPEG medium) unless copper is supplied exogenously (Dancis et al., 1994). As expected, the *ctr1Δctr2Δctr3Δ* cells expressing the empty YES3-Gate vector accumulated 10-fold less copper than the vector-expressing wild type (**Figure 4B**). The expression of *OPT3* in mutant cells increased their copper accumulation by 5-fold compared to the vector expressing cells, although did not bring it to the level of the vector-expressing wild type cells (**Figure 4B**).

Growth of *ctr1*Δ*ctr2*Δ*ctr3*Δ mutant and wild type strains expressing the empty *YES3-Gate* vector and the *ctr1*Δ*ctr2*Δ*ctr3*Δ mutant transformed with *YES3-Gate* with the *OPT3* cDNA insert was also compared on a medium containing non-fermentable carbon sources, ethanol and glycerol (YPEG). The *ctr1*Δ*ctr2*Δ*ctr3*Δ mutant transformed with the *A. thaliana* copper transporter, *COPT2*, was used as an additional positive control (Gayomba et al., 2013). As shown previously, the vector-expressing *ctr1*Δ*ctr2*Δ*ctr3*Δ cells did not grow on YPEG medium even when the medium was supplemented with low (10 and 20 μM) concentration of copper but grew well on YPEG supplemented with 100 μM $CuSO_4$ (**Figure 4C** and (Gayomba et al., 2013)). Unlike *COPT2* expressing cells, *OPT3* expressing mutant cells did not grow on YPEG medium without supplemental copper. However, in contrast to vector expressing *ctr1*Δ*ctr2*Δ*ctr3*Δ cells, *OPT3* expressing cells were able to grow when 10 or 20 μM $CuSO_4$ was added to the medium (**Figure 4C)**. These results are consistent with the role of OPT3 in copper uptake and suggest that, unlike CTR/COPTs, OPT3 might be a low-affinity copper transporter. Together, our results show that OPT3 mainly contributes to the transport of copper ions in heterologous systems.

The *opt3* Mutant is Sensitive to Copper Deficiency.

We next tested the sensitivity of the *opt3* mutant to copper deficiency by comparing its growth and development to the wild type, both grown hydroponically with or without copper supplementation (**Figure 5)**. As we observed previously, the rosette size of the *opt3* mutant was smaller than that in wild type even under control conditions (**Figure 5A** and (Zhai et al., 2014)) and decreased further under copper deficiency *vs.* control conditions; by contrast, copper deficiency did not affect the rosette size of the wild type (**Figure 5A**) early in the vegetative stage of the development. As evidenced by the shorter root length and lower fresh weight of the *opt3* mutant, the increased sensitivity of the *opt3-3* mutant *vs.* wild type to copper deficiency was also observed in seedlings grown on solid medium supplemented with the copper chelator bathocuproine disulfonate (BCS) (**Supplemental Figure S3A, B** and **C online**). Consistent with the increased sensitivity of the *opt3* mutant to copper deficiency and our finding that it experiences copper deficiency, cupric reductase activity was significantly higher in roots of the *opt3* mutant *vs.* wild type (**Supplemental Figure S3D online**).

We then tested whether the transition to flowering is delayed in the *opt3* mutant under control conditions and/or under copper deficiency because we recently found that copper is involved in this process (Rahmati Ishka and Vatamaniuk, 2020). Consistent with our recent findings, wild type plants flowered significantly later and developed more rosette leaves when grown without *vs.* with copper (**Figure 5B** to **D** and **Table 2**). The *opt3* mutant failed to flower within the time frame of the experiment (8 weeks) and developed 30%- and 90% more rosette leaves than wild type in the medium without or with $CuSO_4$, respectively (**Figure 5C, D** and **Table 1**). Leaves of the *opt3* mutant were significantly shorter and were extensively chlorotic compared to wild type, both grown without added copper (**Figure 5E, F**). Although the length of the rosette leaves of mutant and wild type plants was comparable at control copper (125 nM $CuSO_4$), the leaves of the mutant possessed characteristic chlorotic spots (**Figure 5F**). The delayed transition to flowering, the increased number, and the length of rosette leaves of the mutant were rescued by transferring the mutant to the medium with high (500 nM) $CuSO_4$ (**Figure 5C to E, Table 1** and **Supplemental Figure 4A online**). Transferring the mutant to a lower (250 nM) copper also rescued the small size of the mutant, although to a lesser extent compared to high copper (**Supplemental Figure 4B online**).

The *opt3* Mutant Mounts Transcriptional Iron-Deficiency Responses in Roots but not in Shoots.

We next used deep transcriptome sequencing to test whether the expression of copper deficiency-responsive genes is altered in roots, mature and young leaves of the *opt3* mutant compared to wild type. Using Illumina sequencing, we obtained 54, 79 and 59 million clean reads from roots, mature and young leaves, respectively (**Supplemental data set 1**). Of these, 86% reads from roots and mature leaves, and 93% reads from young leaves were mapped to the *A. thaliana* genome and employed to estimate the transcript abundance and differential expression. Compared to wild type, 376, 673 and 1,942 genes were differentially expressed in the *opt3-3* mutant roots, young leaves and mature leaves, respectively (ratio ≥ 1.5 or ≤ 0.67, false-discovery rate [FDR] < 0.05; **Fig. 6A**). As expected, the expression of canonical iron deficiency-responsive genes, known to positively regulate iron-deficiency responses to facilitate iron uptake (*e.g., FIT*, *IRT1*, *FRO2*, *bHLH38*, *bHLH39*, *bHLH100*, *bHLH101*, *MYB10*, *MYB72),* iron-sensing peptide *FEP2/IMA2*, coumarin synthesis and transport (*CYP82C4*, *S8H* and *PDR9/ABCG37*) was highly up-regulated in roots of the *opt3* mutant (**Figure 6B** and **Supplemental Data Set 2**). In addition, IRT1 polypeptide was detected in roots of the *opt3* mutant grown under control conditions and roots of wild type grown under iron deficiency but not in roots of wild type or the *fit-2* mutant grown under control conditions (**Supplemental Figure S5 online**). Of other iron deficiency-regulated genes, the chloroplast-localized *FRO3* and iron exporter *IREG3/FPN3* that is dual-targeted to mitochondria and chloroplast, were also upregulated in roots of the *opt3* mutant compared to the wild type (**Figure 6B** and **Supplemental Data Set 2)**. Of 237 genes upregulated in roots of the *opt3* mutant, 32 were among the robust FIT targets and 6 were among PYE targets (**Supplemental data set 2** and (Mai et al., 2015)), suggesting that the *opt3* mutant mounts primarily FIT-regulated iron deficiency response under iron sufficiency.

Notably, the expression of negative FIT regulators, *ZAT12* and *BTSL1* was upregulated in roots of the *opt3* mutant *vs.* wild type as well (**Figure 6B** and **Supplemental Data Set 2**). In addition, the expression of genes mediating cellular response to iron overload was upregulated. Specifically, the expression of *FER1* encoding a chloroplast-localized iron-sequestering protein, whose expression is upregulated by iron overload to prevent chloroplasts from iron toxicity, was

upregulated in roots of the *opt3* mutant *vs.* wild type (**Figure 6B** and **Supplemental Data Set 2)**. The expression of *IREG2/FPN2*, *VTL1*, *2*, *5* mediating iron sequestration into the vacuole was upregulated too (**Figure 6B** and **Supplemental Data Set 2)**. These data suggest that despite the upregulated FIT-transcriptional network, root cells also perceived the iron-sufficiency/overload signal and responded by increasing the expression of FIT negative regulators and genes involved in the mitigation of iron-overload toxicity.

We then compared the expression of iron-deficiency responsive genes in young and mature leaves of the *opt3* mutant *vs.* wild type. Unlike roots, both mature and young leaves of the *opt3* mutant did not show transcriptional iron deficiency response. Specifically, none of the canonical iron-deficiency upregulated genes were upregulated in young or mature leaves of the *opt3* mutant (**Figure 6B** and **Supplemental Data Set 3 and 4**). Moreover, *FEP1/IMA3*, shown to be involved in iron sensing and typically upregulated in leaves and roots under iron deficiency (Grillet et al., 2018), was downregulated in mature leaves of the *opt3* mutant *vs.* wild type; *At5g05250*, encoding a protein with unknown function, was upregulated by iron deficiency in leaves of different *A. thaliana* ecotypes (Waters et al., 2012), was downregulated in both young and mature leaves of the *opt3* mutant *vs.* wild type. Iron deficiency downregulated genes *NAS3*, *YSL1* and *YSL3* were highly upregulated in mature leaves, and *YSL1* was also upregulated in young leaves of the *opt3* mutant compared to wild type (**Figure 6B** and **Supplemental Data Set 3 and 4**). The chloroplast-localized ferric chelate reductase *FRO7* and plasma membrane-localized *FRO6*, although not regulated by iron deficiency in shoots of *A. thaliana* (Mukherjee et al., 2006), were highly upregulated in mature leaves of the *opt3* mutant *vs.* wild type (**Figure 6B** and **Supplemental Data Set 3**). At the same time, iron-sufficiency markers, *FER1*, *FER3* and *FER4*, were highly upregulated in both mature and young leaves of the *opt3* mutant compared to wild type (**Figure 6B** and **Supplemental Data Set 3 and 4**). Together, our RNA-seq data unraveled the details of contrasting responses of the iron-regulon in roots, young and mature leaves of the *opt3-3* mutant and supported the past observation that leaves of the *opt3* mutants sensed iron overload (Khan et al., 2018).

The *opt3* Mutant Mounts Transcriptional Copper Deficiency Response.

Since roots of the *opt3* mutant accumulated significantly less copper than roots of wild type plants, we predicted that the expression of genes belonging to copper-deficiency regulon in *A.*

thaliana would be altered in the *opt3* mutant as well. Indeed, the expression of canonical copper-deficiency induced genes, responsible for copper uptake (*CITF1*, *COPT2*, *FRO4* and *FRO5*) was up-regulated in roots of the *opt3* mutant compared to wild type (**Table 2, Figure 6B** and **Supplemental Data Set 2**). Also, copper deficiency-repressed genes, contributing to copper economy/metal switch, *CSD1*, *CSD2* and *BCB*, encoding Cu/Zn superoxide dismutases 1 and 2 and blue-copper-binding protein, respectively, were downregulated by more than 2-fold. Consistently, the expression of *FSD1* (Fe-containing superoxide dismutase) was upregulated by 2.7-fold in roots of the *opt3* mutant *vs.* wild type (**Table 2, Figure 6C** and **Supplemental Data Set 2**). In addition, several other canonical copper-deficiency upregulated genes (*bHLH23, ZIP2*, *YSL2*, *TCH4*, *AT2G47010*, *AT4G10500*, *AT1G31710*) were upregulated in roots of the *opt3* mutant compared to wild type (**Table 2, Figure 6B** and **Supplemental Data Set 2)**. Of 16 copper-deficiency regulated genes in the *opt3* mutant, 10 are regarded as SPL7-dependent (**Supplemental Data Set 2)**. These results show that roots of the *opt3-3* mutant manifest molecular symptoms of copper deficiency even though plants were grown under copper-sufficient conditions. These data are consistent with a lower copper concentration in roots of the *opt3* mutant *vs.* wild type (**Figure 2B**).

We also found that young leaves of the *opt3* mutant manifested molecular symptoms of copper deficiency as evident by the increased expression of *YSL1* and *YSL2*, typically upregulated under copper deficiency and involved in lateral movement of minerals including copper (**Figure 6B, C** and **Table 2, Supplemental Data Set 3**). Genes associated with either copper buffering *(MT1A* and *MT2A*) or copper economy (*CSD1*, *CSD2*, *CCS1*, *ARPN*, *UCC2)* were downregulated, while *FSD1* was upregulated (**Figure 6B, C** and **Supplemental Data Set 3**).

Regarding mature leaves, a different set of genes was differentially expressed in the *opt3* mutant *vs.* wild type, and the pattern of the regulation (up- or down-) of canonical copper-deficiency-regulated was not symptomatic for either deficiency or sufficiency (**Supplemental Data Set 4)**. Specifically, as would be expected under copper deficiency, the expression of genes associated with copper uptake and lateral movement, *COPT1*, *YSL1* and *YSL3*, was upregulated in the *opt3-3* mutant *vs.* wild type. Other *A. thaliana* copper-deficiency upregulated genes, including *AT1G32350* and *AT5G02670*, were also upregulated in mature leaves of the *opt3* mutant. Of genes typically downregulated by copper deficiency, *AT4G15660* was also

downregulated in the *opt3* mutant *vs.* wild type as well as *PETE2*, associated with copper sparing and *MT1B*, associated with copper buffering. By contrast, the expression of another copper sink, *UCC2*, typically downregulated by copper deficiency, was upregulated in mature leaves of the *opt3* mutant *vs.* wild type while *NRT2.7*, typically upregulated by copper deficiency in *A. thaliana*, was downregulated in the *opt3* mutant *vs.* wild type.

To conclude, our RNA-Seq data show that both roots and young leaves of the *opt3* mutant mounted transcriptional copper deficiency response while only roots of the mutant manifested transcriptional iron deficiency response.

OPT3 is Transcriptionally Upregulated by the Short-term Copper Deficiency.

While *OPT3* is robustly upregulated in roots and leaves by iron deficiency, it was not found among copper-deficiency-responsive genes in the existing RNA-seq data. In these RNA-seq analyses, plants were exposed to copper deficiency for a minimum of three days. Since *OPT3* responds to iron deficiency within 24 h (Khan et al., 2018), we hypothesized that *OPT3* might also be transcriptionally upregulated by short-term exposure to copper deficiency. Thus, we compared the *OPT3* expression in *A. thaliana* subjected to copper deficiency for 24 or 96 h. We also examined the expression of a copper-deficiency marker, *CITF1*, to validate the efficiency of treatments. *CITF1* was up-regulated in roots by 16-fold after 24 h of copper deficiency and remained highly upregulated after 96 h. The expression of *OPT3* was also upregulated, although to a lesser extent, after 24 h of copper deficiency, but unlike *CITF1*, the transcript abundance of *OPT3* decreased after 96 h of treatment (**Figure 7**). It is noteworthy that the expression of *IRT1* while not upregulated by copper deficiency after 24h, started to increase relative to time 0 after 96h (**Figure 7**).

The Molecular Symptoms of Copper Deficiency in the _opt3_ Mutant are Rescued by Supplemental Copper.

Since transferring the *opt3* mutant to higher copper concentrations decreased its time to flowering to the level of wild type and rescued the length of rosette leaves (**Figure 5** and **Supplemental Fig. 4 online**), we predicted that supplemental copper would also decrease the expression of copper-deficiency responsive genes. To test this hypothesis, we compared the transcript abundance of copper deficiency markers, *CITF1*, *COPT2*, *FRO4* and *FRO5* in roots of

the *opt3* vs. wild type. In parallel, we also tested the expression of key iron deficiency markers, *IRT1* and *FRO2*. Consistent with RNA-seq data (**Table 2**), the expression of *CITF1*, *COPT2*, *FRO4* and *FRO5* was upregulated in roots of the *opt3* mutant *vs.* wild type, both grown under control conditions (**Figure 8)**. The transcript abundance of copper deficiency markers decreased in roots of the *opt3* mutant after transfer to higher concentrations of copper (**Figure 8A** to **H**). We note that transferring wild type plants to higher copper also decreased the expression of *CITF1*, *COPT2*, *FRO4* and *FRO5*, suggesting that 125 nM $CuSO_4$ was somewhat copper limiting even though the growth and development of wild type plants were not affected. Supplemental copper in both concentrations also decreased the expression of *IRT1* and *FRO2* in roots of the *opt3* mutant compared to their expression levels under control conditions (**Figure 8 J to M**). It is noteworthy that high copper (500 nM) increased expression of both *IRT1* and *FRO2* in roots of wild type, reinforcing the existence of interactions between copper and iron homeostasis.

Copper Deficiency Response in Roots of the *opt3* Mutant is Regulated by the Shoot.

We next tested whether the increased expression of copper deficiency markers in roots of the *opt3* mutant is due to its altered shoot-to-root signaling. To do so, we used reciprocal grafting with wild type and *opt3* plants and examined the transcript abundance of copper deficiency markers *CITF1*, *COPT2*, *FRO4*, *FRO5* in roots (**Figure 9)**. The expression of these genes was up-regulated in roots of grafted *opt3*/*opt3* (*opt3* scions grafted to *opt3* rootstocks) compared to the grafted WT/WT (wild type scions grafted with wild type rootstocks [control grafts], **Figure 9A**). The expression of *CITF1*, *COPT2*, *FRO4* and *FRO5* was also elevated in roots of grafts with *opt3* scions and wild type rootstock (**Figure 9A**). In contrast, grafting of the wild type shoots onto the *opt3* rootstocks downregulated *CITF1*, *COPT2*, *FRO4* and *FRO5* expression relative to control grafts (**Figure 9A**). These data shown that the OPT3 function in the shoot is sufficient to regulate the transcriptional copper deficiency responses in the root.

Grafted plants preformed as expected as evidenced by the expression of iron-deficiency markers, *IRT1* and *FRO2* in different graft combinations (**Figure 9B** and (Zhai et al., 2014)). As we showed previously, *IRT1* and *FRO2* were up-regulated in roots of *opt3*/*opt3* compared to WT/WT grafts (**Figure 9B** and (Zhai et al., 2014)). Grafting wild type shoots onto *opt3* mutant roots downregulated *IRT1* and *FRO2* expression relative to their expression in control grafts (**Figure 9B**). In contrast, grafting of *opt3* shoots onto wild type roots increased the expression of

iron deficiency markers (**Figure 9B**). Together, these data show that OPT3 function in the shoot regulates both iron and copper deficiency responses of the root.

Copper and Iron Deficiency Autonomously Regulate the Expression of *CITF1* and *FIT* in Roots of *A. thaliana* Under Simultaneous Copper and Iron Deficiency.

We showed that copper and iron accumulation in the phloem was lower in the *opt3* mutant than in wild type and that OPT3 function is important for regulating copper and iron deficiency responses in the root (**Figures. 1** and **9**). To mimic the effect of simultaneous copper and iron deficiency in the phloem of the *opt3* mutant and its effect on the expression of corresponding deficiency markers in roots, we subjected *A. thaliana* wild type to deficiency of these metals applied concurrently (**Figure 10**). We tested the expression of *CITF1*, because it is highly regulated by copper deficiency and is downregulated by iron deficiency (Yan et al., 2017). We also tested the expression of *FIT* as it is responsive to iron but not copper deficiency (Colangelo and Guerinot, 2004; Bernal et al., 2012). As expected, copper and iron deficiency applied individually had an opposite effect on the expression of *CITF1* (**Figure 10A**); *FIT* expression was upregulated under iron but not copper deficiency (**Figure 10B**). In contrast, the expression of both genes was highly upregulated when iron and copper deficiencies were applied simultaneously (**Figure 10A, B**). This result suggested that iron and copper deficiency applied simultaneously act in parallel/autonomously on the expression of these regulatory genes.

Copper and Iron Deficiency Applied Simultaneously Increase Iron Uptake and Delivery to Shoots.

Because copper deficiency drives iron uptake, we hypothesized that copper deficiency in the *opt3* mutant and its low copper, in addition to low iron, accumulation in the phloem, contributes to iron hyperaccumulation in its roots and leaves. To test this hypothesis, we exposed wild type to copper and iron deficiency individually and concurrently. We then analyzed iron accumulation in roots and leaves of wild type plants. As was found previously, copper deficiency increased iron accumulation in both roots and leaves of *A. thaliana* wild type compared to control conditions (**Figure 10C** and (Bernal et al., 2012; Waters et al., 2012; Kastoori Ramamurthy et al., 2018; Sheng et al., 2021)). As expected, iron accumulation was reduced in both roots and shoots under iron deficiency. Interestingly, the simultaneous application of copper and iron deficiency

increased iron accumulation in both roots and shoots compared to iron deficiency applied individually (**Figure 10C**). We note that plants were subjected to iron deficiency for one week and prior to that they were grown under iron replete conditions. Thus, it is possible that root apoplastic iron reserves were absorbed and accounted for iron accumulation under simultaneous iron and copper deficiencies. We recognize that this experiment does not perfectly match the scenario in the *opt3* mutant that experiences the internal copper and iron deficiency under control conditions. Nevertheless, our results favor the intriguing suggestion that decreased copper accumulation in roots and leaves and the reduced iron and copper accumulation in the phloem contribute to iron overaccumulation in the *opt3* mutant.

Discussion

AtOPT3 Transports Copper and Copper-NA Complex, but Free Copper Ions are Preferred Substrates in the Heterologous System.

The nature of the transport substrate of OPT3 has been under scrutiny and a matter of debates in the literature. OPT3 belongs to the OPT family that is phylogenetically divided into two groups: the Yellow Stripe-Like (YSL) and Oligopeptide Transporter (PT) clades (Lubkowitz, 2011). Analyses of the transport capabilities of some members of *A. thaliana* and *Oryza sativa* OPT family have disclosed their capacity to transport synthetic tetra- and pentapeptides in heterologous systems (Osawa et al., 2006), while members of the YSL clade are expected to transport metal-chelate complexes (Osawa et al., 2006). Given the role of OPT3 in iron homeostasis and signaling, it was expected to transport either peptides that can serve as metal ligands (*e.g.*, glutathione [GSH]) or metal-ligand complexes (*e.g.*, metal-nicotianamine [metal-NA]) (Stacey et al., 2008; Lubkowitz, 2011). Thus, our past finding that OPT3 transports naked ions, iron and cadmium when expressed in *Xenopus* oocytes or the yeast iron uptake mutant, *fet3 fet4* was unexpected (Zhai et al., 2014).

Here, we show that OPT3, in addition to iron and cadmium ions, also transported copper ions when expressed in *Xenopus* oocytes or the *S. cerevisiae* copper transport mutant (**Figure 4**). We also found that OPT3 was able to transport both free copper ions as well as the Cu-NA complex (**Figure 4A**). It is noteworthy, however, that OPT3-expressing oocytes accumulated 4.2 times more copper when it was provided as a free ion rather than complexed with nicotianamine,

suggesting that free copper ions but not Cu-NA complex is a preferred OPT3 substrate in this heterologous system. A recent report has shown that members of the YSL clade of the OPT transporter family, *Brachypodium distachyon* YSL3 and maize YS1 also transport copper ions in *Xenopus* oocytes (Sheng et al., 2021). Unlike AtOPT3, BdYSL3 mediated transport of copper ions but not Cu-NA complex. Similar to AtOPT3, ZmYS1 was capable of transporting both copper ions as well as Cu-NA complexes; similar to AtOPT3, copper ions were the preferred transport substrates of ZmYS1 in the *Xenopus* oocyte heterologous system (Sheng et al., 2021).

Recent *in silico* analysis using protein secondary and tertiary structure simulation and binding affinity results of the docking analyses suggested that AtOPT3 and its counterpart from maize, ZmOPT3 may transport iron complexed with GSH (Kurt, 2021)). Despite this prediction, AtOPT3 does not transport GSH when expressed in the GSH transport mutant, *hgt1*Δ, and the addition of GSH to the *Xenopu*s oocytes bathing medium reduces cadmium transport (Zhai et al., 2014). Our finding that AtOPT3 does not transport GSH in yeast has been recently validated by (Zhang et al., 2016). AtOPT3 counterpart from rice, OsOPT7 is essential for iron homeostasis and sources to sink partitioning but does not transport Fe-NA, Fe-DMA complexes, or GSH in oocytes as well (Bashir et al., 2015). It is noteworthy that unlike AtOPT3, other OPT family members in *A. thaliana*, AtOPT4 and AtOPT6 and the closest OPT3 homolog from *Brassica juncae*, BjGt1 transport GSH (BOGS et al., 2003; Cagnac et al., 2004; Zhang et al., 2016). Recent analyses of the *Arabidopsis opt6* mutant implicated AtOPT6 in GSH long-distance transport and delivery to sink organs, especially flowers (Wongkaew et al., 2018). It is noteworthy that similar to the *opt3* mutant, the loss-of-function of At*OPT6* delays the transition from the vegetative to reproductive stage of the development (Wongkaew et al., 2018). It would be interesting to test whether mineral nutrient homeostasis is disrupted in the *opt6* mutant.

AtOPT3 Mediates Copper (and Iron) Loading to the Phloem for the Delivery to Sink Tissues.

The role of AtOPT3 in iron and copper loading to the phloem for subsequent partitioning from source to sink tissues is evidenced by the decreased accumulation of these metals in the phloem of the *opt3* mutant (**Figures 1E, F; 2A, Supplemental Figure S1 online** and (Zhai et al., 2014)). At the whole plant level, this function of AtOPT3 is important for the phloem-based delivery of copper and iron from sources to sinks, including roots and young leaves (**Figure 2B** and (Zhai et

al., 2014) respectively). Here we also show that AtOPT3 is important for copper and iron delivery to developing embryos and that in addition to leaves, silique valves might act as sources of these minerals for developing seeds (**Figure 3A, B**). This suggestion is based on our findings that silique valves of the mutant hyperaccumulated iron and copper while developing embryos accumulated less iron and copper compared to wild type (**Figure 3 A, B**). We note that unlike copper and iron, manganese and zinc were hyperaccumulated in the vasculature and both silique valves and embryos, while zinc was also hyperaccumulated in seeds of the *opt3* mutant compared to corresponding tissues in wild type (**Figure 1G, H** and **3**). Together, these data suggest that AtOPT3 functions in copper and iron but not manganese and zinc loading to the phloem and the phloem-based delivery to sink tissues.

We note that while the role of AtOPT3 and OsOPT7 in iron delivery to seeds is evidenced by the lower iron concentration in mature seeds (**Figure 3C, D** and (Stacey et al., 2008; Mendoza-Cózatl et al., 2014; Zhai et al., 2014; Bashir et al., 2015), copper accumulation in mature seeds was not affected in the *opt3* mutant (**Figure 3D** and (Stacey et al., 2008)). However, we noted a subtle difference in copper distribution in the mature seed of the *opt3* mutant *vs.* wild type (**Figure 3C**). Specifically, less copper was associated with the vasculature of the *opt3* mutant *vs.* wild type, and somewhat more copper was associated with the seed coat of the mutant (**Figure 3C**). However, this subtle difference in copper distribution was not sufficient to account for total seed concentration.

AtOPT3 Mediates Copper Homeostasis and the *opt3* Mutant Mounts the Transcriptional Copper Deficiency Response in Roots and Young Leaves.

Our finding that OPT3 transports copper in heterologous systems and that the *opt3* mutant accumulates less copper in roots and young leaves compared to wild type (**Figures 2** and **4**) suggested that the mutant might be more sensitive to copper deficiency and/or manifest molecular symptoms of copper deficiency. Indeed, the size of rosette leaves of the *opt3* mutant grown under copper deficiency was significantly smaller compared to control conditions, and its leaves were extensively chlorotic compared to wild type also grown without added copper (**Figure 5A, E** and **F)**. Furthermore, consistent with our recent findings of the role of copper in transition to flowering (Rahmati Ishka and Vatamaniuk, 2020), the *opt3* mutant failed to flower within the time frame of the experiment and developed more rosette leaves than the wild type

when grown in the medium without and even with copper (**Figure 5C, D**). Copper deficiency-associated phenotypes were rescued by transferring the mutant to a medium with higher copper concentrations (**Figure 5C to E** and **Supplemental Figure 4 online**).

In addition, the *opt3* mutant mounted molecular copper-deficiency responses even when it was grown under control conditions. This was evidenced by the increased activity of cupric reductase in roots of the *opt3* mutant *vs.* wild type and the upregulated expression of copper-deficiency regulon in roots and young leaves (**Figure 5** and **Supplemental Datasets 2 to 4**). Changes in the transcriptome of mature leaves of the *opt3* mutant were indicative of neither deficiency nor sufficiency. The transcriptional copper deficiency responses of roots and young leaves and an unspecific response of mature leaves are consistent with their copper accumulation in the corresponding tissues of the *opt3* mutant (**Figures 2, 5** and **Supplemental Datasets 2 to 4**). In addition, our finding of the distinct transcriptional response and metal accumulation in mature *vs.* young leaves of the mutant emphasizes the need to separate these leaves in analyses of mutant phenotypes.

AtOPT3 Mediates Crosstalk Between Iron and Copper Homeostasis and Loss of this Function in the *opt3* Mutant Contributes to Altered Iron Signaling and Iron Overload.

Owing to its well-established role in iron loading into the phloem and iron distribution from sources to sinks, including roots, AtOPT3 is considered to mediate signaling of the shoot iron status to the root (Stacey et al., 2008; Mendoza-Cózatl et al., 2014; Zhai et al., 2014). Thus, the loss of the AtOPT3 function in *opt3* mutant alleles constitutively upregulates *FIT* and the FIT-regulon resulting in iron overaccumulation in roots as well as shoots (**Figure 6 and Supplemental Dataset 2 to 4** and (Stacey et al., 2008; Mendoza-Cózatl et al., 2014; Zhai et al., 2014; Khan et al., 2018)). In contrast to roots, the transcriptome of mature and young leaves reacted to iron overload by upregulating the expression of iron-scavengers, *FER1, FER3, FER4* and genes involved in the redistribution of metal-nicotianamine complexes, *NAS3*, *YSL1* and *YSL3* (**Figure 6 and Supplemental Dataset 2 to 4**).

The distinct expression of *FEP1/IMA3* that we have observed in young and mature leaves of the *opt3* mutant deserves attention (**Figure 6 and Supplemental Dataset 2 to 4**). *FEP1/IMA3* is expressed in the vasculature of roots and leaves, transcriptionally upregulated by iron deficiency, is sufficient to upregulate the expression of the root iron uptake system and is

suggested to function in systemic iron-deficiency signaling (Grillet et al., 2018; Hirayama et al., 2018). We found that *FEP1/IMA3* was downregulated in mature but not young leaves (**Figure 6 and Supplemental Dataset 3** and **4**). This finding suggested that iron is more available in mature leaves than in young leaves since the vasculature of mature but not young leaves perceived iron sufficiency resulting in downregulation of *FEP1/IMA3.* It is important to note that although iron distribution from mature to young leaves is significantly reduced compared to wild type (Zhai et al., 2014), young leaves still accumulated more iron than young leaves of the wild-type (**Supplemental Figure S2 online**). In contrast, young leaves of the *opt3* mutant accumulated significantly less copper while mature leaves accumulated significantly more copper compared to corresponding leaves of the wild type (**Figure 2B**). Furthermore, roots of the *opt3* mutant were also copper deficient (**Figure 2B**). Past findings from different research groups, showing the overaccumulation of iron under copper deficiency in roots and leaves of *A. thaliana*, are especially relevant (**Figure 11A** based on (Bernal et al., 2012; Waters and Armbrust, 2013; Kastoori Ramamurthy et al., 2018; Kroh and Pilon, 2020; Rai et al., 2021; Sheng et al., 2021). These past findings, together with our data showing that AtOPT3, in addition to iron, loads copper to the phloem for redistribution from sources to sinks, invoke the role of AtOPT3 in the regulation of the crosstalk between copper and iron homeostasis and contribute to the understanding of the nature of altered iron deficiency signaling and iron overaccumulation in the *opt3* mutant (**Figure 11B**).

Specifically, we consider two not mutually exclusive and, most likely, concurrent scenarios (**Figure 11B**). 1). A *conservative scenario*: as it was suggested in the past, it is possible that altered iron signaling in the *opt3* mutant due to its inability to load iron to the phloem, causes a constitutive iron deficiency response in the root. As a result, iron overaccumulation occurs in roots and leaves because of the subsequent continual uptake of iron from the outside medium. Considering the signature of the crosstalk between iron and copper, high iron in the *opt3* mutant due to its altered iron deficiency signaling decreases copper uptake, causes copper deficiency and associated molecular signature of copper deficiency. In favor of this scenario are past findings that the accumulation of other metals is significantly altered in the *opt3* mutant (Stacey et al., 2008; Zhai et al., 2014; Khan et al., 2018). 2). *An alternative hypothesis:* the decreased copper accumulation in the phloem of the *opt3* mutant due to its reduced ability to load copper into the phloem, leads to constitutive copper deficiency in young leaves and roots

that, in turn, stimulates iron uptake. In favor of this hypothesis is our finding that the symptoms of copper deficiency and the expression of copper and iron deficiency markers in the *opt3* mutant are rescued by supplemental copper **(Figure 8).** In contrast, the foliar iron application does not rescue the expression of root iron-acquisition genes in the *opt3-2* mutant (Maas et al., 1988; Garcia et al., 2013).

It is most likely that both scenarios occur simultaneously and originate from the function of OPT3 in phloem loading of both copper and iron. The reduced ability to do so in the *opt3* mutant results in a constitutive copper and iron deficiency in the phloem (**Figure 11B**). In support of this suggestion are our data from the grafting experiments showing that wild type shoots grafted onto the *opt3* rootstocks decreased the expression of iron and copper deficiency markers **(Figure 9).** Consistently, the *opt3* scions cause the constitutive upregulation of both iron and copper deficiency marker genes. Furthermore, the simultaneous application of copper and iron deficiency increased iron uptake and delivery to shoots and simulated the expression of copper and iron deficiency markers, *CITF1* and *FIT*, respectively (**Figure 10**).

We also suggest that copper and iron deficiency occurring simultaneously in the phloem of the *opt3* mutant act autonomously in regulating copper and iron deficiency genes. This suggestion is based on the finding that the expression of *CITF1*, normally downregulated by iron deficiency while upregulated by copper deficiency when applied independently, was upregulated under simultaneous application of both deficiencies (**Figure 1A**). Likewise, although *FIT* is upregulated by iron deficiency and does not respond transcriptionally to copper deficiency, it was upregulated by the simultaneous application of copper and iron deficiency (**Figure 10B**).

To conclude, our studies have assigned new functions to AtOPT3 in loading copper into the phloem and subsequent distribution to sink tissues. We have also discovered a role for OPT3 in copper-iron crosstalk that is important for normal homeostasis of both elements. Understanding the basic mechanisms plants use to coordinate iron and copper demands with their uptake, transport and utilization will provide promising avenues for targeted biofortification strategies directed at increasing iron density in the edible portions of crops and improving agricultural productivity on iron and copper-deficient soils.

Materials and Methods

Plant Material and Growth Conditions

Arabidopsis thaliana (*cv*. Col-0) and a previously described *opt3-3* T-DNA insertion mutant (cv. Col-0; SALK_058794C; (Zhai et al., 2014) were obtained from ABRC. Soil-grown plants were directly sown onto Lambert 111 irrigated with regular fertilizer. For copper deficiency treatments, plants were either grown on half-strength Murashige and Skoog (MS) medium (Sigma-Aldrich, M5519) with 1% sucrose and 0.7% agar or hydroponically in a medium containing 1.25 mM KNO_3, 0.625 mM KH2PO_4, 0.5 mM $MgSO_4$, 0.5 mM $Ca(NO_3)$, 10 µM Fe(III)HBED and the following micronutrients: 17.5 µM H_3BO_3, 3.5 µM $MnCl_2$, 0.25 µM $ZnSO_4$, 0.05 µM $NaMoO_4$, 2.5 µM NaCl and 0.0025 µM $CoCl_2$ (Arteca and Arteca 2000), and the indicated concentrations of copper with 125 nM copper considered as control (Yan et al., 2017). For growing plants hydroponically, seeds were surface-sterilized before sowing onto 0.7% (w/v) agar aliquoted in 10 µL pipette tips. Pipette tips were cut before placing them into floats made of foam boards. The roots of seedlings were immersed into the hydroponic solution after 7-8 days of growth. To ensure that both wild type and the *opt3-3* mutant were treated at the same growth stage, all plants were transferred when the rosette reached to 50% of final size (principal growth stage 3.5 as documented in (Boyes et al., 2001)). In this case, wild type and the *opt3-3* plants were transferred 3 and 4 weeks after sowing seeds, respectively. The solution was replaced on a weekly basis and was replaced for one more time 24 hours before collecting samples All plants were grown in a growth chamber at 22℃, 14 h light/10 h dark photoperiod at a photon flux density of 110 µmol m^{-2} s^{-1}.

High-Throughput Sequencing of mRNA, Sequence Mapping and Differential Gene Expression Analysis

A. thaliana wild type and *opt3-3* plants were grown hydroponically with 0.125 µM $CuSO_4$ for 4 weeks. The total RNA was isolated from roots, mature and young leaves using the TRIzol reagent (Invitrogen). The strand-specific RNA-Seq libraries were constructed using 3 µg of total RNA according to procedures described previously (Zhong et al., 2011). RNA-Seq libraries were sequenced on the Illumina HiSeq 2500 system using the single-end mode. Three replicates per sample were used in experiments. Trimmomatic (Bolger et al. 2014) was employed to remove adaptor and low-quality sequences in the Illumina raw reads. Reads shorter than 40 bp were discarded. The resulting reads were aligned to the ribosomal RNA database using Bowtie with 3

mismatches allowed (Langmead et al., 2009; Quast et al., 2013), and those aligned were discarded. The final clean reads were aligned to the Arabidopsis genome sequence (TAIR 10) using TopHat with 1 mismatch allowed (Trapnell et al., 2009). Finally, the counts of mapped reads for each gene model from each sample were derived and normalized to RPKM (reads per kilobase of exon model per million mapped reads). DESeq2 was used to identify differentially expressed genes (DEGs) with the raw count data (Love et al., 2014). Raw *p* values were corrected for multiple testing using the false discovery rate (FDR; (Benjamini and Hochberg, 1995). Genes with an FDR less than 0.05 and fold-changes greater than or equal to 1.5 were regarded as DEGs. GO term enrichment and gene functional classification analyses were performed using Plant MetGenMap (Joung et al., 2009).

ICP-MS Analysis of Copper Concentration in Plant Tissues

Root and shoot tissues were collected from plants grown hydroponically as described above. Iron and other elements were desorbed from root cell walls by washing roots in 10 mM EDTA and a solution with 0.3 mM bathophenanthroline disulphonate (BPS) and 5.7 mM sodium dithionite. The fully expended leaves and the upmost leaves less than 3 mm long were rinsed with deionized water 3 times and then pooled separately as mature leaves and young leaves. The dry seeds and valves were collected from plants grown in soil, and the seeds were separated from the valves with 500 μm mesh. Four to eight plants were pooled for one measurement in each experiment. Three measurements and three independent experiments were conducted. All the samples were dried in an 80°C oven before measuring the weight. Elemental analysis was performed using ICP-MS.

RT-qPCR Analysis

Roots and leaves were collected from plants at Zeitgeber time 7 (Zeitgeber time is defined as the hours after lights-on) and flash-frozen in liquid nitrogen before the homogenization. Total RNA was isolated using TRIzol reagent (Invitrogen) according to the manufacturer's instructions. cDNA templates used for qPCR analysis were synthesized by using AffinityScript QPCR cDNA synthesis kit. One μg of total RNA was treated with DNase I (New England Biolabs) prior to the first-strand cDNA synthesis to eliminate genomic DNA contamination. Real-time PCR analysis was performed in a total volume of 15 mL containing 1x iQSYBR GreenSupermix (Bio-Rad),

500 nM concentration of each PCR primer and 2 µL of 15x diluted cDNA templates using CFX96 real-time PCR system (Bio-Rad) as described (Gayomba et al., 2013). Each experiment was conducted using three independent biological samples, each consisting of 2-3 technical replicates. Data were normalized to the expression of ACTIN2 (AT3G18780). The fold difference (2^{-DDCt}) and the statistical parameters were calculated using the CFX Manager Software, version 3.1 (Bio-Rad).

Grafting Experiments

The grafting method was described previously with slight modification (Marsch-Martínez et al. 2013). All of the procedures were performed under Leica S6E microscope. Briefly, wild type and *opt3-3* seeds were germinated and grown vertically on half-strength MS medium with 0.5% sucrose for 6-7 days. Cotyledons were removed by using sterile scalpels with No.11 blades right before grafting. The scions and rootstocks were then separated and moved to half-strength MS plates with 0.5% sucrose and 0.7% agar for alignment. After grafting, the plants were grown vertically on the plates for another 10 days. Successfully grafted plants without adventitious roots above the graft junction were then transferred to the hydroponic system with 0.25 µM $CuSO_4$ for 24 days before qPCR analysis.

Synchrotron X-Ray Fluorescence Imaging

Fresh samples were detached immediately before the analysis and were placed in a wet chamber made between two layers of metal-free Kaptonfilm, and mounted onto 35-mm slide frames. The spatial distribution of Cu and Fe was imaged via SXRF microscopy at the F3 station at the Cornell High Energy Synchrotron Source (CHESS). The 2D Cu and Fe raster maps were acquired at the 25-µm resolution, 0.2 s/pixel dwell time using a focused, monochromatic incident x-ray beam at 12.8 keV and photon flux of ~10^{10}photons/s. The monochromatic beam was generated with 0.6% energy bandwidth multilayers. Focusing was achieved using a single-bounce moncapillary (named PEB605) fabricated at CHESS. These settings did not cause detectable damage to plant tissues within the 6- to 9-h scans required for analysis of the full set of samples. Element-specific x-ray fluorescence was detected using a Vortex ME-4 silicon drift detector. Quantifications were done by calibrating using a thin metal foil film standard during each experiment and concentrations were expressed as µg cm^{-2}. Data was processed with the

software Praxes, which was developed at CHESS and employs PyMCA libraries in batch mode (Solé et al., 2007).

Synchrotron-based Confocal XRF Microscopy

Confocal XRF experiments were obtained at beamline 5-ID (SRX). The beamline monochromator and focusing optics were employed to deliver $3x10^{11}$ photons/second in a 1x1 μm^2 beam, with incident beam energy of 10.0 keV and bandwidth of approximately 1 eV. The confocal geometry was achieved by placing a collimating channel array (CCA) (Agyeman-Budu et al., 2016) onto a single-element Vortex SDD detector perpendicular to the beam. The sample stage was oriented such that the horizontal translation axis of the stage is 35 degrees from that of the incident beam, and 55 degrees from the detector axis. The particular CCA employed for these measurements has a series of 175, 2-µm channels etched into a 1-mm thick Germanium substrate, etched to an approximate depth of 300 µm. The working distance between the sample and optic is 1.5 mm. Due to the finite width of the optic at its front tip, the maximum probe depth of the system in this configuration is 0.8 mm. Quantitative calibration of the confocal XRF system was achieved by methods described in (Malzer and Kanngießer, 2005; Mantouvalou et al., 2012).

Synchrotron-based X-ray Fluorescence Computed Microtomography (F-CMT)

Internal distributions of copper, iron and other micronutrient elements in wild type and the *opt3-3* mutant seeds were measured *in vivo* by synchrotron-based X-ray Fluorescence Computed Microtomography (F-CMT) at the X-ray Fluorescence Microprobe (XFM) beamline at the National Synchrotron Light Source II (NSLS-II) in Upton, NY. XFM (4-BM) beamline is designed for monochromatic operation in the 2.3 to 23 keV range and optimized for high-quality, spatially-resolved X-ray absorption spectroscopy (Sulfur to Technetium K-edges) in conjunction with element-specific imaging and microdiffraction. XFM beamline can also be operated in a pink beam “imaging” mode that delivers a 1-micron spot with up to 1000X more flux than the XFM monochromatic beam. XFM filtered pink beam (12 – 20 keV broadband) was focused by Kirkpatrick-Baez (KB) mirrors to a 1-micron spot for F-CMT measurements of seeds. Seeds were mounted to a quartz post that interfaces with a Huber goniometer head on a rotation stage attached to a fast-scanning translation stage. F-CMT images were acquired at the seed center by rotating and translating the specimen in the microbeam while recording the fluorescence

intensities with a Hitachi 4-element Vortex SDD coupled to Quantum Detectors Xspress3 electronics. F-CMT data were collected using 0.75 – 3.0° degree angular steps, 2 – 8 µm translation steps and 50 ms dwell time. Tomographic image reconstructions using a conventional filtered back projection algorithm were processed using tomo-Py plugin to GSE Mapviewer in the LARCH package (Newville, 2013). The image intensity scale for mutant lines was adjusted to match the wild type control.

Copper Uptake in *Xenopus laevis* Oocytes

The basal uptake solution consisted of a modified ND96 solution containing 96 mM NaCl, 1 mM KCl, 0.9 mM $CaCl_2$, buffered with 5 mM 2-(N-morpholino) ethanesulfonic acid/NaOH to pH 6.0, as previous studies determined these conditions were suitable to minimize endogenous transport in oocytes (Zhai et al., 2014). The uptake solution was supplemented with 100 µM Cu-NA or 100 µM $CuSO_4$. Each sample contained 8 – 10 oocytes, with 5 replicates per data point. At a given time point, the uptake was terminated by washing oocytes six consecutive times with an ice-cold basal uptake solution. Oocytes were collected and samples were digested in 100 µL of 70% HClO4, re-suspended in 5 ml of 0.1 M nitric acid, and analyzed using inductively coupled plasma mass spectrometry (Sciex ICP-MS).

Functional Complementation Assays in *Saccharomyces cerevisiae*.

S. cerevisiae SEY6210 (*MATa ura3-52 leu2-3,-112 his3Δ200 trp1Δ901 lys2-801 suc2Δ9*) wild type and the *ctr1Δctr2Δctr3Δ* triple mutant (*MATa ura3-52 his3Δ200 trp1-901 ctr1*::*ura3*::*Knr ctr2*::*HIS3 ctr3*::*TRP1*) were used for functional complementation assays. *YES3-Gate-OPT3* construct or *YES3-Gate* lacking the cDNA insert were transformed into appropriate yeast line using the Frozen-EZ Yeast Transformation II kit (Zymo Research). Transformants were selected for uracil prototrophy on YNB medium containing 6.7% (w/v) yeast nitrogen base without amino acids (Difco), 0.77% (w/v) CSM-URA, 0.5% (w/v) NaCl, 2% glucose, 2% (w/v) agar.

Functional complementation assays included analyses of the respiration competence and copper accumulation in yeast cells as described (Jung et al., 2012). Specifically, the respiration competence of different cell lines was tested by the ability of cells to grow on non-fermentable carbon sources (Dancis et al., 1994). To do so, different cell lines transformed with *YES3-Gate* with or without *OPT3* cDNA insert were grown in liquid YNB-URA to an $OD_{600\ nm}$ = 1.0,

serially 10-fold diluted, and spotted onto YPEG medium containing 1% (w/v) yeast extract, 2% (w/v) bacto-peptone, 3% (v/v) glycerol, 2% (v/v) ethanol, and 2% (w/v) agar and the indicated concentrations of $CuSO_4$. Plates were incubated for 3 days at 30°C.

To analyze copper accumulation, different yeast lines were grown to exponential log phase in liquid YNB media described above. An aliquot (150 µl) of the overnight grown culture was inoculated into 20 ml of the fresh YNB media with 40 µg/L $CuSO_4$ and cells were grown at 30°C. After 24 h, cells were collected by centrifugation, washed with deionized water before copper was desorbed from yeast cell wall followed by washings in desorbing buffer containing 1mM EDTA and 100 µM of a copper chelator, bathocuproine disulfonate BCS, pH8.0. Cells were then washed two more times in de-ionized water and collected by centrifugation. The cell pellet was dried, digested by heating with a combination of purified concentrated nitric and perchloric acids, and finally dissolved in 10 ml of 5% nitric acid. The concentration of copper in processed yeast cells was analyzed by inductively coupled plasma mass spectroscopy (ICP-MS; Agilent 7500).

Collection and Analysis of Phloem Sap

Phloem sap was collected from wild type and *opt3-3* mutant plants grown hydroponically at the late vegetative stage as described (Zhai et al., 2014). Briefly, leaf numbers 9 and 10 collected from one plant were pooled together, and the xylem sap was flashed by placing the petioles in a tube filled with 300 µL of deionized water and incubated in an illuminated growth chamber for 15 min followed by further incubation in darkness for 1 h. The petioles were then recut in 5 mM Na_2-EDTA (pH 7.5) under low light before placing the petioles in 250 µL of 5 mM Na_2-EDTA (pH 7.5). Leaves were then incubated in darkness for 1 h in a high-humidity chamber lined with wet paper towels and sealed with Vaseline. Samples were diluted with 5 mL of 5% HNO_3 for subsequent detection of K or Cu by ICP-MS.

Statistical analysis

Statistical analyses of experimental data were performed using the ANOVA single-factor analysis and Tukey HSD using JMP® Pro 14 (SAS Institute Inc., Cary, NC, 1989-2007).

Accession numbers

Sequence data of the genes from this article can be found in the Arabidopsis Genome Initiative or GenBank/EMBL databases under the following accession numbers: *OPT3* (AT4G16370), *CITF1* (AT1G71200), *FRO4* (AT5G23980), FRO5 (AT5G23990), *COPT1* (AT5G59030), *COPT2* (AT3G46900), *YSL1* (AT4G24120), *YSL2* (AT5G24380), *YSL3* (AT5G53550), *CSD1* (AT1G08830), *CSD2* (AT2G28190), *IRT1* (AT4G19690), *FRO2* (AT1G01580), *FRO6* (AT5G49730), *FRO7* (AT5G49740), *FSD1* (AT4G25100), *ARPN* (AT2G02850), *BCB* (AT5G20230), *CCS1* (AT1G12520), *UCC2* (AT2G44790), *FER1* (AT5G01600), *FER3* (AT3G65090), *FER4* (AT2G40300), *ZIP2* (AT5G59520), *bHLH23* (AT4G28790), TCH4 (AT5G57560), *BTSL1* (AT1G74770), *ZAT12* (AT5G59820), *FEP2/IMA2* (AT1G47395), *FEP1/IMA3* (AT2G30766), *IREG2/FPN2* (AT5G03570), *VTL1* (AT1G21140), *VTL2* (AT1G76800), *VTL5* (AT3G25190), *NAS3* (AT1G09240), *PETE2* (AT1G20340), *MT1B* (AT5G56795), *NRT2.7* (AT5G14570), *MT1B* (AT5G56795), *MT1A* (AT1G07600), *MT2A* (AT3G09390), *AT2G47010, AT4G10500, At1G31710, At1G32350, At5G02670,* and *At5g05250*.

Author Contributions and Acknowledgements:

J-C. C. and O. K. V. designed experiments; all authors contributed to different experiments presented in this manuscript. J.C. and O. K. V. wrote the manuscript with contribution from all authors. We thank Mary Lou Guerinot (Dartmouth, USA) for providing seed of the *fit-2* mutant and for constructive comments on the manuscript. We thank a former member of the Vatamaniuk lab, Nanditha Vimalakumari for her contribution to Figure 4 and all current lab members for constructive comments on the manuscript. We thank Dr. John Grazul at the Cornell Center for Materials Research (CCMR) for assisting in preparation samples for 2D-CXRF. The CCMR facility is supported by the National Science Foundation under Award Number DMR-1719875. Parts of this research used the XFM and SRX Beamlines of the National Synchrotron Light Source II, a U.S. Department of Energy (DOE) Office of Science User Facility operated for the DOE Office of Science by Brookhaven National Laboratory under Contract No. DE-SC0012704. This work is based upon research conducted at the Cornell High Energy Synchrotron Source (CHESS), which during the period of research was supported by the National Science Foundation under award DMR-1332208; the Center for High Energy X-ray Sciences (CHEXS) is presently supported by the National Science Foundation under award

DMR-1829070. This study was funded by NSF-IOS #1656321 to O. K. V. and NSF-IOS #1754966 to E. W., O. K. V. and M. P.

References

Agyeman-Budu DN, Choudhury S, Coulthard I, Gordon R, Hallin E, Woll AR (2016) Germanium Collimating micro-Channel Arrays For High Resolution, High Energy Confocal X-ray Fluorescence Microscopy. Icxom23: International Conference on X-Ray Optics and Microanalysis 1764

Alexander SPH, Kelly E, Mathie A, Peters JA, Veale EL, Armstrong JF, Faccenda E, Harding SD, Pawson AJ, Sharman JL, et al. (2019) THE CONCISE GUIDE TO PHARMACOLOGY 2019/20: Transporters. British Journal of Pharmacology 176: S397-S493

Araki R, Mermod M, Yamasaki H, Kamiya T, Fujiwara T, Shikanai T (2018) SPL7 locally regulates copper-homeostasis-related genes in Arabidopsis. J Plant Physiol 224-225: 137-143

Bashir K, Ishimaru Y, Itai RN, Senoura T, Takahashi M, An G, Oikawa T, Ueda M, Sato A, Uozumi N, et al. (2015) Iron deficiency regulated OsOPT7 is essential for iron homeostasis in rice. Plant Molecular Biology 88: 165-176

Baxter IR, Vitek O, Lahner B, Muthukumar B, Borghi M, Morrissey J, Guerinot ML, Salt DE (2008) The leaf ionome as a multivariable system to detect a plant's physiological status. Proceedings of the National Academy of Sciences 105: 12081-12086

Benjamini Y, Hochberg Y (1995) Controlling the False Discovery Rate: A Practical and Powerful Approach to Multiple Testing. Journal of the Royal Statistical Society. Series B (Methodological) 57: 289-300

Bernal M, Casero D, Singh V, Wilson GT, Grande A, Yang H, Dodani SC, Pellegrini M, Huijser P, Connolly EL, et al. (2012) Transcriptome sequencing identifies SPL7-regulated copper acquisition genes FRO4/FRO5 and the copper dependence of iron homeostasis in Arabidopsis. Plant Cell 24: 738-761

Bernal M, Casero D, Singh V, Wilson GT, Grande A, Yang H, Dodani SC, Pellegrini M, Huijser P, Connolly EL, et al. (2012) Transcriptome Sequencing Identifies SPL7-Regulated Copper Acquisition Genes FRO4/FRO5 and the Copper Dependence of Iron Homeostasis in Arabidopsis. The Plant Cell Online 24: 738-761

Bernal M, Casero D, Singh V, Wilson GT, Grande A, Yang H, Dodani SC, Pellegrini M, Huijser P, Connolly EL, et al. (2012) Transcriptome Sequencing Identifies SPL7 -Regulated Copper Acquisition Genes FRO4 FRO5 and the Copper Dependence of Iron Homeostasis in Arabidopsis The Plant Cell 24: 738-761

BOGS J, BOURBOULOUX A, CAGNAC O, WACHTER A, RAUSCH T, DELROT S (2003) Functional characterization and expression analysis of a glutathione transporter, BjGT1, from Brassica juncea: evidence for regulation by heavy metal exposure. Plant, Cell & Environment 26: 1703-1711

Broadley M, Brown P, Cakmak I, Rengel Z, Zhao F (2012) Chapter 7 - Function of Nutrients: Micronutrients A2 - Marschner, Petra. *In* Marschner's Mineral Nutrition of Higher Plants (Third Edition). Academic Press, San Diego, pp 191-248

Burkhead JL, Gogolin Reynolds KA, Abdel-Ghany SE, Cohu CM, Pilon M (2009) Copper homeostasis. New Phytologist 182: 799-816

Cagnac O, Bourbouloux A, Chakrabarty D, Zhang MY, Delrot S (2004) AtOPT6 transports glutathione derivatives and is induced by primisulfuron. Plant Physiology 135: 1378-1387

Chang CJ (2015) Searching for harmony in transition-metal signaling. Nat Chem Biol 11: 744-747

Chen C, Galon Y, Rahmati Ishka M, Malihi S, Shimanovsky V, Twito S, Rath A, Vatamaniuk OK, Miller G (2020) ASCORBATE PEROXIDASE6 delays the onset of age-dependent leaf senescence. Plant Physiology

Colangelo EP, Guerinot ML (2004) The essential basic helix-loop-helix protein FIT1 is required for the iron deficiency response. Plant Cell 16: 3400-3412

Cui Y, Chen CL, Cui M, Zhou WJ, Wu HL, Ling HQ (2018) Four IVa bHLH Transcription Factors Are Novel Interactors of FIT and Mediate JA Inhibition of Iron Uptake in Arabidopsis. Mol Plant 11: 1166-1183

Dancis A, Haile D, Yuan DS, Klausner RD (1994) The Saccharomyces cerevisiae copper transport protein (Ctr1p). Biochemical characterization, regulation by copper, and physiologic role in copper uptake. J Biol Chem 269: 25660-25667

Epstein E, Bloom A (2005) Mineral nutrition of plants: principles and perspectives, 2nd eds. Sunderland, Mass Sinaur: 292-305

Gao F, Robe K, Bettembourg M, Navarro N, Rofidal V, Santoni V, Gaymard F, Vignols F, Roschzttardtz H, Izquierdo E, et al. (2020) The Transcription Factor bHLH121 Interacts with bHLH105 (ILR3) and Its Closest Homologs to Regulate Iron Homeostasis in Arabidopsis. Plant Cell 32: 508-524

Garcia MJ, Romera FJ, Stacey MG, Stacey G, Villar E, Alcantara E, Perez-Vicente R (2013) Shoot to root communication is necessary to control the expression of iron-acquisition genes in Strategy I plants. Planta 237: 65-75

Gayomba SR, Jung H-i, Yan J, Danku J, Rutzke MA, Bernal M, Kramer U, Kochian LV, Salt DE, Vatamaniuk OK (2013) The CTR/COPT-dependent copper uptake and SPL7-dependent copper deficiency responses are required for basal cadmium tolerance in A. thaliana. Metallomics 5: 1262-1275

Gayomba SR, Jung HI, Yan J, Danku J, Rutzke MA, Bernal M, Kramer U, Kochian LV, Salt DE, Vatamaniuk OK (2013) The CTR/COPT-dependent copper uptake and SPL7-dependent copper deficiency responses are required for basal cadmium tolerance in A. thaliana. Metallomics 5: 1262-1275

Gayomba SR, Zhai Z, Jung HI, Vatamaniuk OK (2015) Local and systemic signaling of iron status and its interactions with homeostasis of other essential elements. Front Plant Sci 6: 716

Grillet L, Lan P, Li W, Mokkapati G, Schmidt W (2018) IRON MAN is a ubiquitous family of peptides that control iron transport in plants. Nat Plants 4: 953-963

Ha JH, Doguer C, Wang X, Flores SR, Collins JF (2016) High-Iron Consumption Impairs Growth and Causes Copper-Deficiency Anemia in Weanling Sprague-Dawley Rats. PLoS One 11: e0161033

Hirayama T, Lei GJ, Yamaji N, Nakagawa N, Ma JF (2018) The Putative Peptide Gene FEP1 Regulates Iron Deficiency Response in Arabidopsis. Plant Cell Physiol 59: 1739-1752

Jain A, Wilson G, Connolly E (2014) The diverse roles of FRO family metalloreductases in iron and copper homeostasis. Frontiers in Plant Science 5

Jeong J, Merkovich A, Clyne M, Connolly EL (2017) Directing iron transport in dicots: regulation of iron acquisition and translocation. Curr Opin Plant Biol 39: 106-113

Jiang A, Guo Z, Pan J, Zhuang Y, Zuo D, Hao C, Gao Z, Xin P, Chu J, Zhong S, et al. (2020) The *PIF1-MIR408-Plantacyanin* Repression Cascade Regulates Light Dependent Seed Germination. bioRxiv: 2020.2007.2020.212340

Joung J-G, Corbett AM, Fellman SM, Tieman DM, Klee HJ, Giovannoni JJ, Fei Z (2009) Plant MetGenMAP: An Integrative Analysis System for Plant Systems Biology. Plant Physiology 151: 1758-1768

Jung H-i, Gayomba SR, Rutzke MA, Craft E, Kochian LV, Vatamaniuk OK (2012) COPT6 is a plasma membrane transporter that functions in copper homeostasis in Arabidopsis and is a novel target of SQUAMOSA promoter-binding protein-like 7. The Journal of biological chemistry 287: 33252-33267

Jung HI, Gayomba SR, Rutzke MA, Craft E, Kochian LV, Vatamaniuk OK (2012) COPT6 is a plasma membrane transporter that functions in copper homeostasis in *Arabidopsis* and is a novel target of SQUAMOSA promoter-binding protein-like 7. J Biol Chem 287: 33252-33267

Kastoori Ramamurthy R, Xiang Q, Hsieh EJ, Liu K, Zhang C, Waters BM (2018) New aspects of iron-copper crosstalk uncovered by transcriptomic characterization of Col-0 and the copper uptake mutant spl7 in Arabidopsis thaliana. Metallomics 10: 1824-1840

Khan MA, Castro-Guerrero NA, McInturf SA, Nguyen NT, Dame AN, Wang J, Bindbeutel RK, Joshi T, Jurisson SS, Nusinow DA, et al. (2018) Changes in iron availability in Arabidopsis are rapidly sensed in the leaf vasculature and impaired sensing leads to opposite transcriptional programs in leaves and roots. Plant, Cell & Environment 41: 2263-2276

Khan MA, Castro-Guerrero NA, McInturf SA, Nguyen NT, Dame AN, Wang J, Bindbeutel RK, Joshi T, Jurisson SS, Nusinow DA, et al. (2018) Changes in iron availability in Arabidopsis are rapidly sensed in the leaf vasculature and impaired sensing leads to opposite transcriptional programs in leaves and roots. Plant Cell Environ 41: 2263-2276

Kim SA, LaCroix IS, Gerber SA, Guerinot ML (2019) The iron deficiency response in *Arabidopsis thaliana* requires the phosphorylated transcription factor URI. Proceedings of the National Academy of Sciences 116: 24933-24942

Kim SA, Punshon T, Lanzirotti A, Li L, Alonso JM, Ecker JR, Kaplan J, Guerinot ML (2006) Localization of Iron in Arabidopsis Seed Requires the Vacuolar Membrane Transporter VIT1. Science 314: 1295-1298

Klevay LM (2001) Iron overload can induce mild copper deficiency. J Trace Elem Med Biol 14: 237-240

Kobayashi T (2019) Understanding the Complexity of Iron Sensing and Signaling Cascades in Plants. Plant Cell Physiol 60: 1440-1446

Kroh GE, Pilon M (2020) Micronutrient homeostasis and chloroplast iron protein expression is largely maintained in a chloroplast copper transporter mutant. Funct Plant Biol 47: 1041-1052

Kumar RK, Chu H-H, Abundis C, Vasques K, Rodriguez DC, Chia J-C, Huang R, Vatamaniuk OK, Walker EL (2017) Iron-Nicotianamine Transporters Are Required for Proper Long Distance Iron Signaling Plant Physiology 175: 1254-1268

Kumar RK, Chu HH, Abundis C, Vasques K, Rodriguez DC, Chia JC, Huang R, Vatamaniuk OK, Walker EL (2017) Iron-Nicotianamine Transporters Are Required for Proper Long Distance Iron Signaling. Plant Physiol 175: 1254-1268

Kurt F (2021) An Insight into Oligopeptide Transporter 3 (OPT3) Family Proteins. Protein and Peptide Letters 28: 43-54

Langmead B, Trapnell C, Pop M, Salzberg SL (2009) Ultrafast and memory-efficient alignment of short DNA sequences to the human genome. Genome Biology 10: R25

Li WF, Lan P (2017) The Understanding of the Plant Iron Deficiency Responses in Strategy I Plants and the Role of Ethylene in This Process by Omic Approaches. Frontiers in Plant Science 8

Love MI, Huber W, Anders S (2014) Moderated estimation of fold change and dispersion for RNA-seq data with DESeq2. Genome Biology 15: 550

Lubkowitz M (2011) The Oligopeptide Transporters: A Small Gene Family with a Diverse Group of Substrates and Functions? Mol Plant 4: 407-415

Maas FM, van de Wetering DA, van Beusichem ML, Bienfait HF (1988) Characterization of phloem iron and its possible role in the regulation of Fe-efficiency reactions. Plant Physiol 87: 167-171

Mai HJ, Lindermayr C, von Toerne C, Fink-Straube C, Durner J, Bauer P (2015) Iron and FER-LIKE IRON DEFICIENCY-INDUCED TRANSCRIPTION FACTOR-dependent regulation of proteins and genes in Arabidopsis thaliana roots. Proteomics 15: 3030-3047

Malzer W, Kanngießer B (2005) A Model for the Confocal Volume of 3D Micro X-ray Fluorescence Spectrometer. Spectrochimica Acta Part B: Atomic Spectroscopy 60: 1334-1341

Mantouvalou I, Malzer W, Kanngießer B (2012) Quantification for 3D micro X-ray fluorescence. Spectrochimica Acta Part B: Atomic Spectroscopy 77: 9-18

Mantouvalou I, Malzer W, Kanngiesser B (2012) Quantification for 3D micro X-ray fluorescence. Spectrochimica Acta Part B-Atomic Spectroscopy 77: 9-18

Mendoza-Cózatl DG, Xie Q, Akmakjian GZ, Jobe TO, Patel A, Stacey MG, Song L, Demoin DW, Jurisson SS, Stacey G, et al. (2014) OPT3 is a component of the iron-signaling network between leaves and roots and misregulation of OPT3 leads to an over-accumulation of cadmium in seeds. Mol Plant 7: 1455-1469

Mukherjee I, Campbell NH, Ash JS, Connolly EL (2006) Expression profiling of the Arabidopsis ferric chelate reductase (FRO) gene family reveals differential regulation by iron and copper. Planta 223: 1178-1190

Newville M (2013) Larch: An Analysis Package for XAFS and Related Spectroscopies. J. Phys.: Conf. Ser. 430

Osawa H, Stacey G, Gassmann W (2006) ScOPT1 and AtOPT4 function as proton-coupled oligopeptide transporters with broad but distinct substrate specificities. Biochemical Journal 393: 267-275

Pottier M, Dumont J, Masclaux-Daubresse C, Thomine S (2019) Autophagy is essential for optimal translocation of iron to seeds in Arabidopsis. Journal of experimental botany 70: 859-869

Quast C, Pruesse E, Yilmaz P, Gerken J, Schweer T, Yarza P, Peplies J, Glöckner FO (2013) The SILVA ribosomal RNA gene database project: improved data processing and web-based tools. Nucleic Acids Research 41: 7

Rahmati Ishka M, Vatamaniuk OK (2020) Copper deficiency alters shoot architecture and reduces fertility of both gynoecium and androecium in Arabidopsis thaliana. BioRxiv

Rahmati Ishka M, Vatamaniuk OK (2020) Copper deficiency alters shoot architecture and reduces fertility of both gynoecium and androecium in Arabidopsis thaliana. Plant Direct 4: e00288

Rai S, Singh PK, Mankotia S, Swain J, Satbhai SB (2021) Iron homeostasis in plants and its crosstalk with copper, zinc, and manganese. Plant Stress 1: 100008

Ravet K, Danford FL, Dihle A, Pittarello M, Pilon M (2011) Spatiotemporal Analysis of Copper Homeostasis in Populus trichocarpa Reveals an Integrated Molecular Remodeling for a Preferential Allocation of Copper to Plastocyanin in the Chloroplasts of Developing Leaves. Plant Physiology 157: 1300-1312

Ravet K, Pilon M (2013) Copper and Iron Homeostasis in Plants: The Challenges of Oxidative Stress. Antioxidants & Redox Signaling 19: 23

Rees EM, Lee J, Thiele DJ (2004) Mobilization of Intracellular Copper Stores by the Ctr2 Vacuolar Copper Transporter. Journal of Biological Chemistry 279: 54221-54229

Rodríguez FI, Esch JJ, Hall AE, Binder BM, Schaller GE, Bleecker AB (1999) A Copper Cofactor for the Ethylene Receptor ETR1 from *Arabidopsis*. Science 283: 996-998

Schott-Verdugo S, Müller L, Classen E, Gohlke H, Groth G (2019) Structural Model of the ETR1 Ethylene Receptor Transmembrane Sensor Domain. Scientific Reports 9: 8869

Schwarz B, Bauer P (2020) FIT, a regulatory hub for iron deficiency and stress signaling in roots, and FIT-dependent and -independent gene signatures. J Exp Bot 71: 1694-1705

Shahbaz M, Ravet K, Peers G, Pilon M (2015) Prioritization of copper for the use in photosynthetic electron transport in developing leaves of hybrid poplar. Frontiers in Plant Science 6

Sheng H, Jiang Y, Ishka MR, Chia J-C, Dokuchayeva T, Kavulych Y, Zavodna T-O, Mendoza PN, Huang R, Smieshka LM, et al. (2021) YSL3-mediated copper distribution is required for fertility, grain yield, and size in *Brachypodium*. Plant Physiology: 2019.2012.2012.874396

Sheng H, Jiang Y, Ishka MR, Chia JC, Dokuchayeva T, Kavulych Y, Zavodna TO, Mendoza PN, Huang R, Smieshka LM, et al. (2021) YSL3-mediated copper distribution is required for fertility, seed size and protein accumulation in Brachypodium. Plant Physiol 186: 655-676

Solé VA, Papillon E, Cotte M, Walter P, Susini J (2007) A multiplatform code for the analysis of energy-dispersive X-ray fluorescence spectra. Spectrochimica Acta Part B: Atomic Spectroscopy 62: 63-68

Spielmann J, Vert G (2020) The many facets of protein ubiquitination and degradation in plant root iron-deficiency responses. Journal of Experimental Botany 72: 2071-2082

Stacey MG, Koh S, Becker J, Stacey G (2002) AtOPT3, a Member of the Oligopeptide Transporter Family, Is Essential for Embryo Development in Arabidopsis. The Plant Cell 14: 2799-2811

Stacey MG, Patel A, McClain WE, Mathieu M, Remley M, Rogers EE, Gassmann W, Blevins DG, Stacey G (2008) The Arabidopsis AtOPT3 Protein Functions in Metal Homeostasis and Movement of Iron to Developing Seeds. Plant Physiology 146: 589-601

Trapnell C, Pachter L, Salzberg SL (2009) TopHat: discovering splice junctions with RNA-Seq. Bioinformatics 25: 7

Tsang T, Posimo JM, Gudiel AA, Cicchini M, Feldser DM, Brady DC (2020) Copper is an essential regulator of the autophagic kinases ULK1/2 to drive lung adenocarcinoma. Nature cell biology 22: 412-424

Turski ML, Brady DC, Kim HJ, Kim BE, Nose Y, Counter CM, Winge DR, Thiele DJ (2012) A novel role for copper in Ras/mitogen-activated protein kinase signaling. Mol Cell Biol 32: 1284-1295

Turski ML, Thiele DJ (2009) New roles for copper metabolism in cell proliferation, signaling, and disease. J Biol Chem 284: 717-721

Waters BM, Armbrust LC (2013) Optimal copper supply is required for normal plant iron deficiency responses. Plant Signal Behav 8: e26611

Waters BM, McInturf SA, Amundsen K (2014) Transcriptomic and physiological characterization of the fefe mutant of melon (Cucumis melo) reveals new aspects of iron-copper crosstalk. New Phytol 203: 1128-1145

Waters BM, McInturf SA, Stein RJ (2012) Rosette iron deficiency transcript and microRNA profiling reveals links between copper and iron homeostasis in Arabidopsis thaliana. J Exp Bot 63: 5903-5918

Wongkaew A, Asayama K, Kitaiwa T, Nakamura SI, Kojima K, Stacey G, Sekimoto H, Yokoyama T, Ohkama-Ohtsu N (2018) AtOPT6 Protein Functions in Long-Distance Transport of Glutathione in Arabidopsis thaliana. Plant and Cell Physiology 59: 1443-1451

Wu Y, Zhang D, Chu Jee Y, Boyle P, Wang Y, Brindle Ian D, De Luca V, Després C (2012) The Arabidopsis NPR1 Protein Is a Receptor for the Plant Defense Hormone Salicylic Acid. Cell Reports 1: 639-647

Yamasaki H, Hayashi M, Fukazawa M, Kobayashi Y, Shikanai T (2009) SQUAMOSA Promoter Binding Protein-Like7 Is a Central Regulator for Copper Homeostasis in *Arabidopsis*. Plant Cell 21: 347-361

Yan J, Chia J-C, Sheng H, Jung H-i, Zavodna T-O, Zhang L, Huang R, Jiao C, Craft EJ, Fei Z, et al. (2017) Arabidopsis Pollen Fertility Requires the Transcription Factors CITF1 and SPL7 That Regulate Copper Delivery to Anthers and Jasmonic Acid Synthesis. The Plant Cell 29: 3012-3029

Zhai Z, Gayomba SR, Jung H-I, Vimalakumari NK, Piñeros M, Craft E, Rutzke MA, Danku J, Lahner B, Punshon T, et al. (2014) OPT3 Is a Phloem-Specific Iron Transporter That Is Essential for Systemic Iron Signaling and Redistribution of Iron and Cadmium in Arabidopsis. The Plant cell 26: 2249-2264

Zhai Z, Gayomba SR, Jung H-i, Vimalakumari NK, Piñeros M, Craft E, Rutzke MA, Danku J, Lahner B, Punshon T, et al. (2014) OPT3 is a phloem-specific iron transporter that is essential for systemic iron signaling and redistribution of iron and cadmium in Arabidopsis. Plant Cell 26: 2249-2264

Zhang Z, Xie Q, Jobe TO, Kau AR, Wang C, Li Y, Qiu B, Wang Q, Mendoza-Cózatl DG, Schroeder JI (2016) Identification of AtOPT4 as a Plant Glutathione Transporter. Mol Plant 9: 481-484

Zhong S, Joung J-G, Zheng Y, Chen Y-r, Liu B, Shao Y, Xiang JZ, Fei Z, Giovannoni JJ (2011) High-Throughput Illumina Strand-Specific RNA Sequencing Library Preparation. Cold Spring Harbor Protocols 2011: pdb.prot5652

Figure Legends

Figure 1. Iron and copper distribution is altered in the vasculature of the *opt3* mutant.
Plants were grown hydroponically with 250 nM $CuSO_4$ for 26 days (in **A** to **D**) or for 5 weeks (in **E** to **H**) before tissues were collected. **A** to **D** show 2D XRF maps of the indicated minerals in mature leaves; **E** to **H** show 2D-CXRF maps of indicated elements in f the vasculature of mature leaves petioles. Bars = 1 mm; Xy and Ph indicate the location of the xylem and the phloem, respectively.

Figure 2. AtOPT3 mediates copper loading to the phloem and redistribution from mature leaves to young leaves and roots.
The concentration of copper in the phloem sap (**A**) and the indicated plant tissues (**B**) of wild type and the *opt3* mutant. Plants were grown hydroponically under iron and copper sufficient conditions. Shown values are arithmetic means ± S.E. Asterisks indicate statistically significant differences from wild type ($p < 0.05$, Student's *t* test, n = 3 to 4 experiments).

Figure 3. The *opt3* mutant accumulates less copper and iron in developing embryos and seeds.
ICP-MS analysis of mineral accumulation in dry silique valves (**A**) and seeds (**D**) collected from soil-grown plants. Shown values are arithmetic means ± S.E. Asterisks indicate statistically significant differences from wild type ($p < 0.05$, Student's *t* test, n = 3 independent experiments with tissues pooled from four to five plants per experiment). **B**. Fifteen-mm-long developing siliques were collected from soil-grown plants and subjected to 2D-SXRF analysis. White arrows point to embryos **C**. Dry seeds were collected as described for A and D and subjected to 2D CT-XRF. Blue arrows point to the vasculature, blue boxes to regions in the seed coat with contrasting copper accumulation. **B** and **C** show representative images of at least three scanned specimens.

Figure 4. OPT3 transports copper in *X. laevis* oocytes and *S. cerevisiae*
(**A**) Copper uptake into X*enopus* oocytes injected with either *OPT3* cRNA (**OPT3**) or water (**Moc**k). Copper uptake was measured at 3 h. The basal uptake solution was supplemented with

100 µM $CuSO_4$ (**Cu^{2+}**) or 100 µM Cu-NA (**Cu-NA**). Presented values are arithmetic means ± S.E. (n = 5). Asterisks indicate statistically significant differences (**, $p < 0.01$, using Student's *t*-test). **(B)** Copper concentration in *S. cerevisiae* wild-type, SEY6210 and its isogenic *ctr1*Δ*2*Δ*3*Δ mutant both expressing the empty *YES3-Gate* vector (***Wt*** and ***ctrΔ***, respectively) or the *ctr1*Δ*2*Δ*3*Δmutant expressing *YES3-Gate-OPT3* (**OPT3**). Levels not connected with the same letter are statistically different (n = 4 to 5, Tukey HSD test). (**C**) The wild type and the *ctr1*Δ*2*Δ*3*Δ *S. cerevisiae* mutant transformed with the empty YES3-Gate vector or the *ctr1*Δ*2*Δ*3*Δ transformed with the vector containing the *OPT3* cDNA or the *A. thaliana* copper transporter, *COPT2*, were serially 10-fold diluted and spotted onto solid YPEG medium supplemented with different concentrations of $CuSO_4$. Colonies were visualized after incubating plates for 3 days at 30°C. Dilution series are indicated on the right. *S. cerevisiae* lines were designated as in (**B**) except that ***OPT3-1*** and ***OPT3-2*** designate two distinct *OPT3* expressing clones that were selected and propagated after yeast transformation).

Figure 5. The *opt3* mutant is sensitive to copper deficiency.

In (**A**) and (**B**), wild type and the *opt3* mutant were grown hydroponically with or without 125 nM $CuSO_4$ (+ Cu or – Cu, respectively). Images were taken after 4 weeks (**A**) or 9 weeks (**B**) from the seed sowing. (**C**), (**D**) and (**E**) show time to flowering, primary rosette leaf number and leaf length, respectively. Plants were germinated and growth hydroponically without or with copper (**0** or **125**, respectively and **white bars**). After four weeks of growth, a subset of plants grown with or without copper was transferred to 500 nM $CuSO_4$ (**500** and **grey bars**). Measurements were taken after one week of growth and when plants were eight-week-old. Data show mean values ± S.E. Levels not connected by the same letter are statistically different (Tukey HSD, JMP Pro 14 software package, n = 3 independent experiments with data collected from 3 to 6 plants per each experiment). (**F**) shows a representative image of leaves (from young to old in the direction from left to right) of wild type and the *opt3* mutant both grown hydroponically for 4 weeks with or without copper (**125 nM Cu** or **0 nM Cu**, respectively).

Figure 6. The *opt3* mutant mounts copper deficiency response in roots and young leaves.

A. Total number of differentially expressed genes in roots, mature leaves and young leaves of the *opt3* mutant vs wild type, according to RNA-seq data (ratio >= 1.5 or <=0.67, false-discovery

rate [FDR] < 0.05). Venn diagrams show the number of upregulated (**B**) or downregulated (**C**) genes in roots, mature and young leaves. Overlaps indicate the number of genes co-regulated in indicated tissues. Genes associated with iron and copper homeostasis are shown in (**B**) and (**C**). Genes involved in copper homeostasis are marked in bold; genes associated with both iron and copper deficiency responses are marked in bold and underlined.

Figure 7. The expression of *OPT3* is upregulated by copper deficiency.

Four-week-old plants grown hydroponically with 250 nM $CuSO_4$ and a subset of plants was transferred to a fresh medium without copper. Roots were collected after 1 or 4 days of treatments for RT-qPCR analysis. *CITF1* was used as a marker of copper deficiency to validate the efficiency of treatment. Shown are mean values ± S.E. Asterisks indicate statistically significant differences from the expression of genes under control condition, set to one ($p < 0.05$, Student's *t* test, n = 3 independent experiments).

Figure 8. Copper supplementation partially rescues the molecular symptoms of copper deficiency in the *opt3* mutant.

Plants were grown hydroponically under control conditions (**white bars**) until the late-vegetative stage before a subset of plants was transferred to a fresh medium with higher copper concentrations (250 nM $CuSO_4$, **light grey bars** in **A, B, E, F, J, K** or 500 nM $CuSO_4$, **dark grey bars** in **C, D, G, H, L, M**). Plants were grown for another week prior to tissue collection and RT-qPCR analysis. The transcript abundance of indicated genes was normalized to the wild type grown under control conditions. Data show mean values ± S.E. Levels not connected by the same letter are statistically different (Tukey HSD, JMP Pro 14 software package, n= 3 independent experiments with roots pooled from 3 plants per each experiment).

Figure 9. The expression of copper deficiency markers is controlled by the OPT3 function in the shoot.

The transcript abundance of copper- (**A**) and iron-deficiency (**B**) markers in roots of grafted plants. Wild type and the *opt3* mutant were used for reciprocal grafting. **Wt*S*/Wt*R*,** wild type scion grafted to wild type rootstock (control); ***opt3S/opt3R***, *opt3* scion grafted to *opt3* rootstock; **Wt*S*/opt3*R***, wild type scion grafted to *opt3* rootstock; ***opt3S/WtR***, *opt3* scion grafted to wild

type rootstock. Shown values represent means ± S.E. Asterisks (*) indicate statistically significant values of the expression level is > 2 or <0.5 compared to control grafts ($p < 0.05$, based on CFX Manager 3.1 (BIO-RAD). Shown data are representative of three independent experiments.

Figure 10. Copper and iron deficiency applied simultaneously increase the expression of *CITF1* and *FIT*, iron uptake and delivery to shoots.

The transcript abundance of *CITF1* (**A**) and *FIT* (**B**) and iron concentration in roots (**C**) were analyzed in roots of plants grown under control conditions (**Ctr**) or without cooper but with iron (**–Cu**) for four weeks prior to tissue collection. To achieve iron deficiency, plants were grown under control conditions for three weeks, transferred to a solution without iron and grown for one additional week (**–Fe**). For the simultaneous iron and copper deficiency treatment, plants were grown without copper but with iron for three weeks and then transferred to a fresh hydroponic medium lacking both copper and iron. Tissues were collected and analysed after an additional week of growth (**–Cu – Fe**). Mean values ± S.E are shown. Levels not connected by the same letter are statistically different (Tukey HSD, JMP Pro 14 software package, n = 3 independent experiments with roots pooled from 3 plants per each experiment).

Figure 11. Altered Fe-Cu crosstalk in the *opt3* mutant contributes to iron over-accumulation. As illustrated in (**A**), iron deficiency in the outside medium causes copper accumulation in roots and leaves of *A. thaliana* wild type while copper deficiency in the outside medium results in iron accumulation (Bernal et al., 2012; Waters et al., 2012; Waters and Armbrust, 2013; Waters et al., 2014). By contrast, high iron status can repress copper accumulation in *A. thaliana* (Waters and Armbrust, 2013)**.** This has been also documented in animal species (Klevay, 2001; Ha et al., 2016). In the *opt3* mutant (**B**) the scenario is different in that, although both iron and copper are available in the outside medium, the *opt3* mutant experiences simultaneous iron and copper deficiency in the phloem (**Low Fe in the phloem; Low Cu in the Phloem**, respectively). Low iron accumulation in the phloem stimulates transcriptional iron deficiency response and iron accumulation since iron is available in the outside medium. Copper deficiency in the phloem, roots and leaves also lead to iron accumulation and transcriptional copper deficiency response. Increased iron accumulation from both pathways, in turn, decreases copper uptake further altering Fe-Cu crosstalk.

Supplemental Figure S1. Copper accumulation in the phloem exudates of wild type and the *opt3* mutant. Error bars indicate S.E. Asterisks indicate statistically significant differences from wild type ($p < 0.05$, Student's t test). A minimum of ten replicates per sample were performed. Plants were grown and phloem sap collected as described in (Kumar et al., 2017).

Supplemental Figure S2. The *opt3* mutant accumulates high concentration of metals in vegetative tissues.

Plants were grown hydroponically with 125 nM (**A**) or 250 nM $CuSO_4$ (**B**) for 30 days prior to tissue collection for ICP-MS analysis. Shown values are arithmetic means ± S.E. Asterisks indicated statistically significant differences from wild type ($p < 0.05$, Student's *t* test, n = 3 independent experiments. In each experiment, tissues were pooled from four to five plants per measurement).

Supplemental Figure S3. Seedlings of the *opt3* mutant are sensitive to copper deficiency.

Plants were grown on ½ MS solid medium with or without 200 µM or 500 µM of a copper chelator BCS. (**A**) shows a representative image of plants after 10 days of growth after which root length (**B**), fresh weight (**C**) and cupric reductase activity (**D**) were analyzed. In **B** to **D** data are means ± S.E. Levels not connected by the same letter are significantly different ($p < 0.05$, Tukey-Kramer HSD test). In **B**, n = 3 independent experiments with the root length analyzed from 88 seedlings; in **C,** n = 3 independent experiments with 30 to 40 seedlings in each experiment; in **D**, n = 3 independent experiments with 20 seedlings analyzed in each experiment.

Supplemental Figure S4. Transferring the *opt3* mutant to high copper rescues its growth.

(**A**) Wild type and the *opt3* mutant were germinated and grown hydroponically 125 nM Cu for 4 weeks before transferring to a fresh hydroponic medium with 500 nM (**A**) or 250 nM (**B**) copper. Images were taken after one week of growth.

Supplemental Figure S5. The *opt3* mutant accumulates IRT1 protein in roots under Fe sufficient growth conditions.

(**A**) Western blots analysis of IRT1 protein accumulation in roots of wild type and the *opt3-3* mutant. Plants were grown hydroponically with 125 nM $CuSO_4$ and 10 mM Fe-HBED for 4 weeks prior to tissues collection. (**B**) Western blots analysis of iron deficiency-induced IRT1 accumulation in wild type roots. Plants were grown hydroponically with 125 nM $CuSO_4$ and 10 µM Fe-HBED for 3 weeks and then transferred to a fresh medium without iron. Roots were collected after one week of growth under iron deficiency. The *fit-2* mutant was incorporated as a negative control for the IRT1 protein accumulation. In (**A**) and (**B**), the IRT1 signals are recognized by the antibody at 35 kD while actin (protein loading control) at 45 kD. For the immunodetection of actin epitope, the nitrocellulose blots were probed with the primary mouse-monoclonal anti-actin antibody (1:5,000 dilution, Sigma-Adrich) and secondary, an HRP-conjugated goat-antimouse IgG antibody (1:10,000 Rockland Immunochemicals). In both cases, immunoreactive bands were visualized with Clarity Max ECL blotting substrates (BIORAD).

Table 1. Average day from the date of sawing to flowering in wild type and the *opt3-3* mutant grown hydroponically with 0 or 125 nM $CuSO_4$. A subset of plants was shifted to 500 nM copper[1].

	Cu concentrations, nM			
Genotype	**0**	**0 to 500**	**125**	**125 to 500**
Wild type (Col-0)	46.83 ± 2.86	40.17 ± 0.79	42.33 ± 0.76	41.80 ± 1.24
opt3-3 (Col-0)	N.A.[2]	48 ± 1.78	N.A.[2]	48.4 ± 1.80

[1] data showing average ± standard errors (n = 3 to 6)

[2] NA; not applicable. The mutant did not flower during the course of measurements which ranged from week 5 to week 8.

Table 2. Expression of copper deficiency-responsive genes in roots, mature leaves and young leaves of the *opt3-3* mutant. Upregulated or downregulated genes are shown in red or blue bold font, respectively, and marked with asterisks (ratio >= 1.5 or <=0.67, [FDR] < 0.05).

AGI ID	Gene	Short description	RPKM*						Ratio (*opt3-3*/wt)			Ratio (*YL vs ML*†)	
			*opt3*_R†	wt_R†	*opt3*_ML†	wt_ML†	*opt3*_YL†	wt_YL†	R†	ML†	YL†	Wt	opt3
AT5G59030	*COPT1*	Cu transporter 1	7.28	3.46	164.42	98.92	68.26	60.38	2.1	**1.7***	1.1	**0.6***	**0.4***
AT3G46900	*COPT2*	Cu transporter 2	183.29	46.13	1.57	1.96	0.36	0.11	**4.0***	0.8	3.3	**0.1***	**0.2***
AT2G26975	*COPT6*	Cu transporter 6	0.3	0.28	38.02	26.09	16.48	17.73	1.1	1.5	0.9	0.7*	**0.4***
AT4G24120	*YSL1*	YELLOW STRIPE like 1	0.15	0.35	10.39	3.32	4.33	2.54	0.4	**3.1***	**1.7***	0.8	**0.4***
AT5G24380	*YSL2*	YELLOW STRIPE like 2	19.19	10.3	1.47	0.97	1.31	0.47	**1.9***	0.7	**2.8***	**0.5***	0.9
AT5G53550	*YSL3*	YELLOW STRIPE like 3	19.26	20.51	20.96	11.63	8.17	8.56	0.9	**1.8***	1.0	0.7*	**0.4***
AT5G23980	*FRO4*	Ferric reduction oxidase 4	221.4	103.4	5.6	8.7	0.6	0.8	**2.1***	0.7	0.7	**0.1***	**0.1***
AT5G23990	*FRO5*	Ferric reduction oxidase 5	326.7	39.5	0.5	0.7	0.1	0.0	**8.3***	0.8	NA	**0.2***	**0.1***
AT1G71200	*CITF1*	Cu-inducible transcription factor 1	9.6	1.5	0.0	0.0	0.0	0.0	**6.6***	NA	NA	1.0	0.3
AT1G08830	*CSD1*	Cu/Zn superoxide dismutase 1	100.0	243.4	69.3	102.0	28.2	181.1	**0.4***	0.7	**0.2***	1.8	**0.4***
AT2G28190	*CSD2*	Cu/Zn superoxide dismutase 2	72.7	123.3	68.8	151.0	138.6	452.8	**0.6***	0.5	**0.3***	**3.0***	2.0
AT2G02850	*ARPN*	Plantacyanin; copper ion binding protein	17.9	19.6	0.7	0.7	2.2	6.5	0.9	1.0	**0.3***	**9.8***	**3.3***
AT5G20230	*BCB*	Blue copper binding protein	1.4	3.6	258.6	325.8	41.3	110.8	**0.4***	0.8	0.4	**0.3***	**0.2***
AT1G12520	*CCS1*	Cu chaperone for superoxide dismutase 1	32.7	55.8	18.6	20.9	12.5	39.4	**0.6***	0.9	**0.3***	1.9	**0.7***
AT2G44790	*UCC2*	UCLACYANIN 2; Cu ion binding protein	1068.8	1418.9	4.5	1.9	1.3	4.4	0.8*	**2.4***	**0.3***	2.3	**0.3***
AT4G25100	*FSD1*	Fe superoxide dismutase 1	331.9	120.9	807.2	584.7	681.3	264.0	**2.7***	1.4	**2.6***	**0.5***	0.8*
AT3G56240	*CCH*	CCH (Cu chaperone)	242.96	171.84	103.78	96.9	42.55	39.82	1.4*	1.1	1.1	**0.4***	**0.4***
AT1G71040	*LPR2*	LPR2 (Low Phosphate Root2); Cu ion binding	30.11	30.98	102.9	83.53	35.62	43.25	1.0	1.2	0.8	**0.5***	**0.4***
AT2G07687		Cytochrome *c* oxidase subunit 3	1.14	2.26	1.03	1.29	0.26	0.7	0.5	0.8	0.4	0.5	**0.3***
AT1G18140	*LAC1*	LAC1 (Laccase 1); copper ion binding /oxidoreductase	2.44	2.92	0.03	0.01	0.39	0.98	0.8	NA	0.4	**98***	**14.6***
AT2G29130	*LAC2*	LAC2 (Laccase 2); Cu ion binding /oxidoreductase	22.42	28.28	0.06	0.3	0.44	0.95	0.8	0.2	0.5	3.2	**7.4***
AT2G46570	*LAC6*	LAC6 (Laccase 6); Cu ion binding /oxidoreductase	2.57	2.55	0.7	0.38	3.23	3.15	1.0	1.8	1.0	**8.2***	**4.6***

RPKM stands for Reads Per Kilobase of transcript per Million mapped reads. Asterisks (, $P < 0.05$) indicate transcript levels which are significantly different between wild type and *opt3-3* mutant.

†R, roots; ML, mature leaves, YL, young leaves.

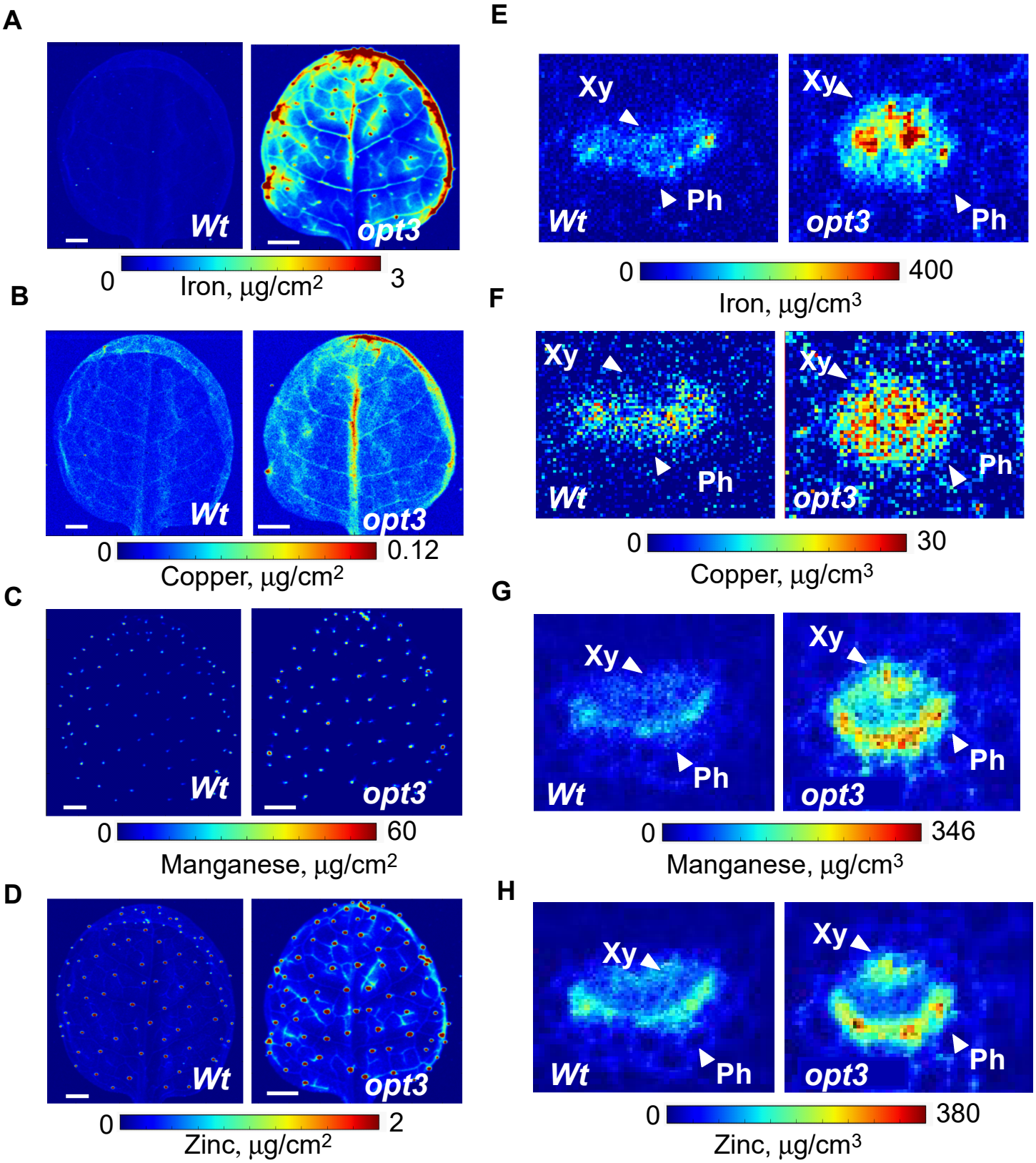

Figure 1. Iron and copper distribution is altered in the vasculature of the *opt3* mutant.

Plants were grown hydroponically with 250 nM $CuSO_4$ for 26 days (in **A** to **D**) or for 5 weeks (in **E** to **H**) before tissues were collected. **A** to **D** show 2D XRF maps of the indicated minerals in mature leaves; **E** to **H** show 2D-CXRF maps of indicated elements in the vasculature of mature leaf petioles. Bars = 1 mm; Xy and Ph indicate the location of the xylem and the phloem, respectively.

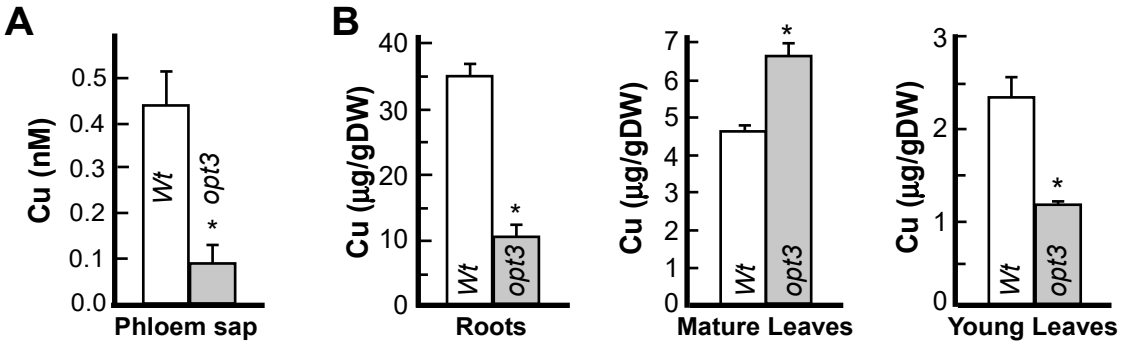

Figure 2. AtOPT3 mediates copper loading to the phloem and redistribution from mature leaves to young leaves and roots.

The concentration of copper in the phloem sap (**A**) and the indicated plant tissues (**B**) of wild type and the *opt3* mutant. Plants were grown hydroponically under iron and copper sufficient conditions. Shown values are arithmetic means ± S.E. Asterisks indicate statistically significant differences from wild type ($p < 0.05$, Student's *t* test, n = 3 to 4 experiments).

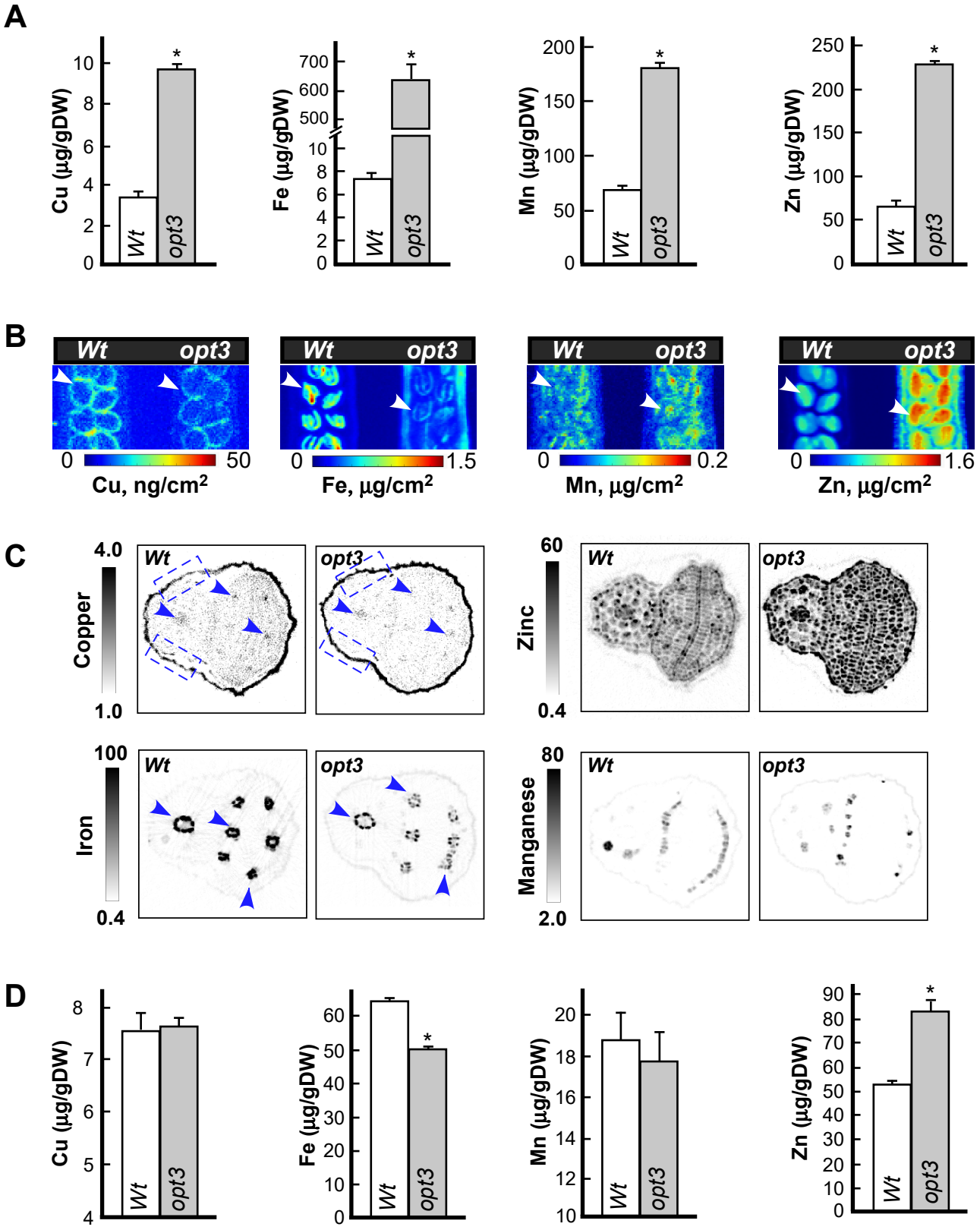

Figure 3. The *opt3* mutant accumulates less copper and iron in developing embryos and seeds.

ICP-MS analysis of mineral accumulation in dry silique valves (**A**) and seeds (**D**) collected from soil-grown plants. Shown values are arithmetic means ± S.E. Asterisks indicate statistically significant differences from wild-type ($p < 0.05$, Student's *t* test, n = 3 independent experiments with tissues pooled from four to five plants per experiment). **B**. Fifteen-mm-long developing siliques were collected from soil-grown plants and subjected to 2D-SXRF analysis. White arrows point to embryos in **C**. Dry seeds were collected as described for **A** and **D** and subjected to 2D CT-XRF. Blue arrows point to the vasculature, blue boxes to regions in the seed coat with contrasting copper accumulation. **B** and **C** show representative images of at least three scanned specimens.

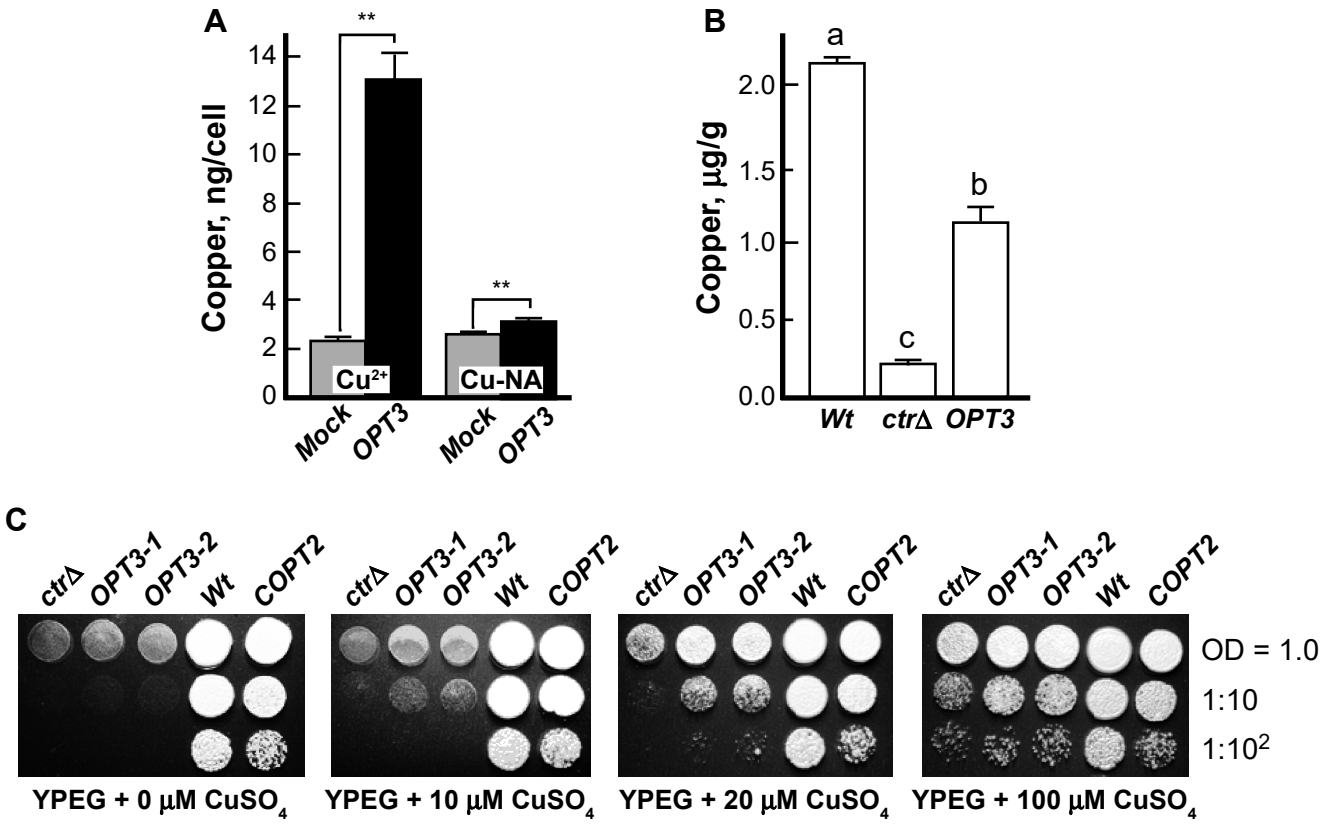

Figure 4. OPT3 transports copper in *X. laevis* oocytes and *S. cerevisiae.*

(**A**) Copper uptake into X*enopus* oocytes injected with either *OPT3* cRNA (**OPT3**) or water (**Moc**k). Copper uptake was measured at 3 h. The basal uptake solution was supplemented with 100 µM $CuSO_4$ (**Cu^{2+}**) or 100 µM Cu-NA (**Cu-NA**). Presented values are arithmetic means ± S.E. (n = 5). Asterisks indicate statistically significant differences (**, $p < 0.01$, using Student's *t*-test). **(B)** Copper concentration in *S. cerevisiae* wild type, SEY6210 and its isogenic *ctr1*Δ*2*Δ*3*Δ mutant both expressing the empty *YES3-Gate* vector (***Wt*** and ***ctr*Δ**, respectively) or the *ctr1*Δ*2*Δ*3*Δ mutant expressing *YES3-Gate-OPT3* (**OPT3**). Levels not connected with the same letter are statistically different (n = 4 to 5, Tukey HSD test). (**C**) The wild type and the *ctr1*Δ*2*Δ*3*Δ *S. cerevisiae* mutant transformed with the empty YES3-Gate vector or the *ctr1*Δ*2*Δ*3*Δ transformed with the vector containing the *OPT3* cDNA or the *A. thaliana* copper transporter, *COPT2*, were serially 10-fold diluted and spotted onto solid YPEG medium supplemented with different concentrations of $CuSO_4$. Colonies were visualized after incubating plates for 3 days at 30°C. Dilution series are indicated on the right. *S. cerevisiae* lines were designated as in (**B**) except that ***OPT3-1*** and ***OPT3-2*** designate two distinct *OPT3* expressing clones that were selected and propagated after yeast transformation).

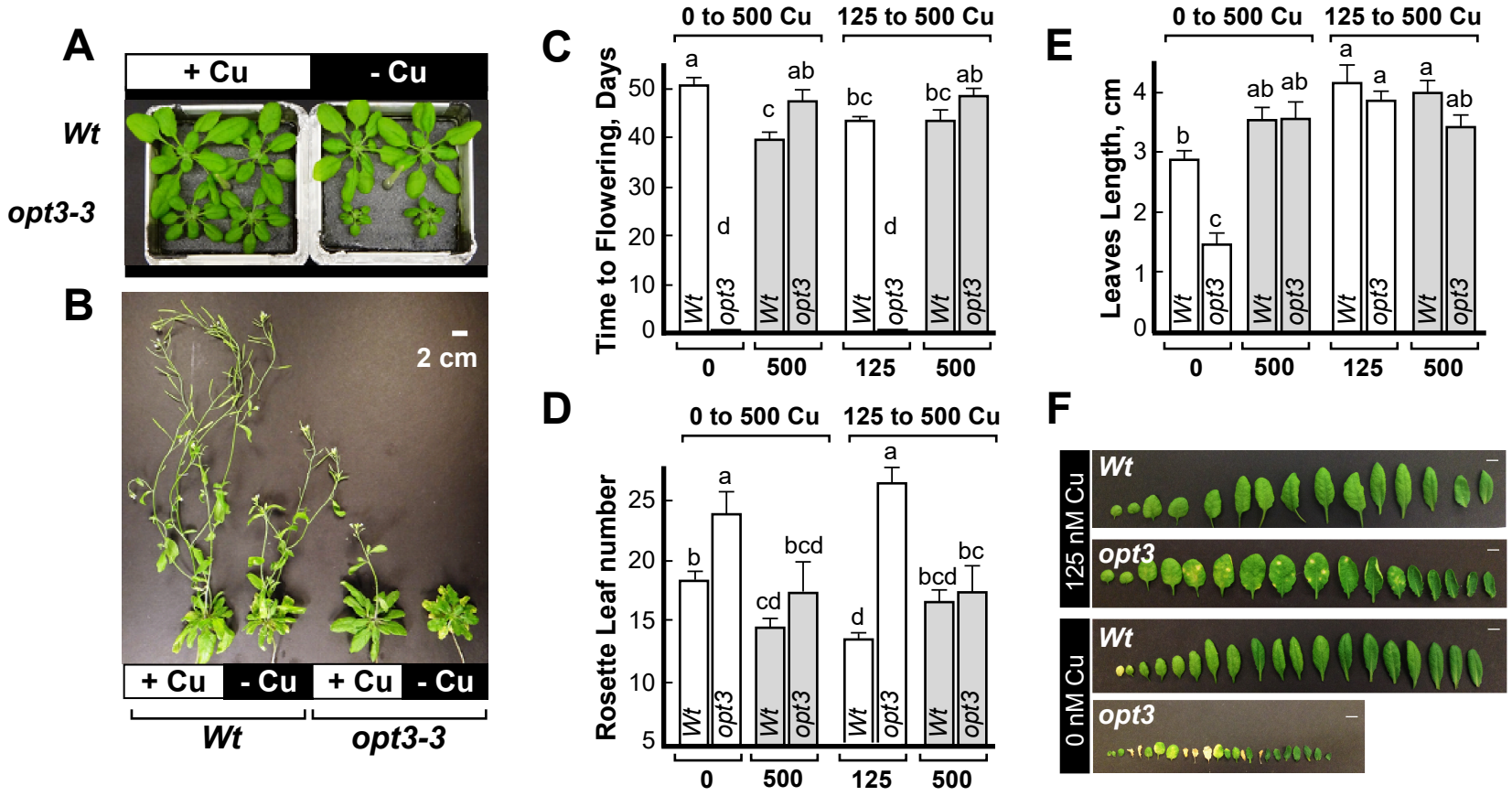

Figure 5. The *opt3* mutant is sensitive to copper deficiency.

In (**A**) and (**B**), wild type and the *opt3* mutant were grown hydroponically with or without 125 nM $CuSO_4$ (+ Cu or – Cu, respectively). Images were taken after 4 weeks (**A**) or 9 weeks (**B**) from the seed sowing. (**C**), (**D**) and (**E**) show time to flowering, primary rosette leaf number and leaf length, respectively. Plants were germinated and growth hydroponically without or with copper (**0** or **125**, respectively and **white bars**). After four weeks of growth, a subset of plants grown with or without copper was transferred to 500 nM $CuSO_4$ (**500** and **grey bars**). Measurements were taken after one week of growth and when plants were eight-week-old. Data show mean values ± S.E. Levels not connected by the same letter are statistically different (Tukey HSD, JMP Pro 14 software package, n = 3 independent experiments with data collected from 3 to 6 plants per each experiment). (**F**) shows a representative image of leaves (from young to old in the direction from left to right) of wild type and the *opt3* mutant both grown hydroponically for 4 weeks with or without copper (**125 nM Cu** or **0 nM Cu**, respectively).

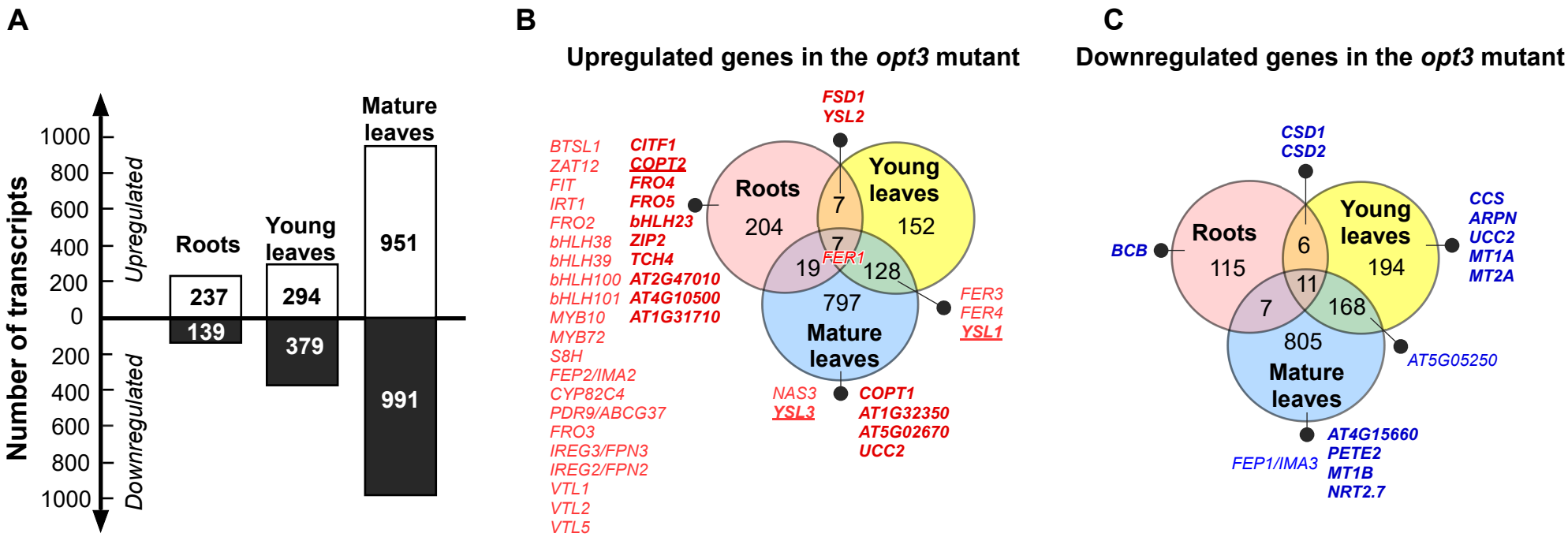

Figure 6. The *opt3* mutant mounts copper deficiency response in roots and young leaves.

A. Total number of differentially expressed genes in roots, mature leaves and young leaves of the *opt3* mutant *vs.* wild type, according to RNA-seq data (ratio >= 1.5 or <=0.67, false-discovery rate [FDR] < 0.05). Venn diagrams show the number of upregulated (**B**) or downregulated (**C**) genes in roots, mature and young leaves. Overlaps indicate the number of genes co-regulated in indicated tissues. Genes associated with iron and copper homeostasis are shown in (**B**) and (**C**). Genes involved in copper homeostasis are marked in bold; genes associated with both iron and copper deficiency responses are marked in bold and underlined.

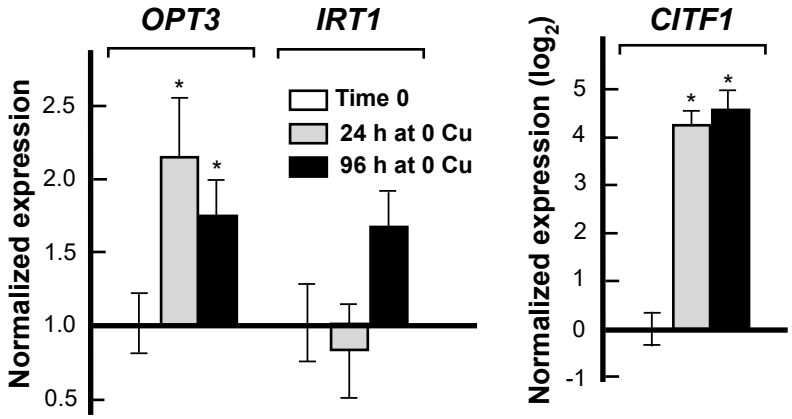

Figure 7. The expression of *OPT3* is upregulated by copper deficiency.

Four-week-old plants grown hydroponically with 250 nM $CuSO_4$ and a subset of plants was transferred to a fresh medium without copper. Roots were collected after 1 or 4 days of treatments for RT-qPCR analysis. *CITF1* was used as a marker of copper deficiency to validate the efficiency of treatment. Shown are mean values ± S.E. Asterisks indicate statistically significant differences from the expression of genes under control condition, set to one ($p < 0.05$, Student's *t* test, n = 3 independent experiments).

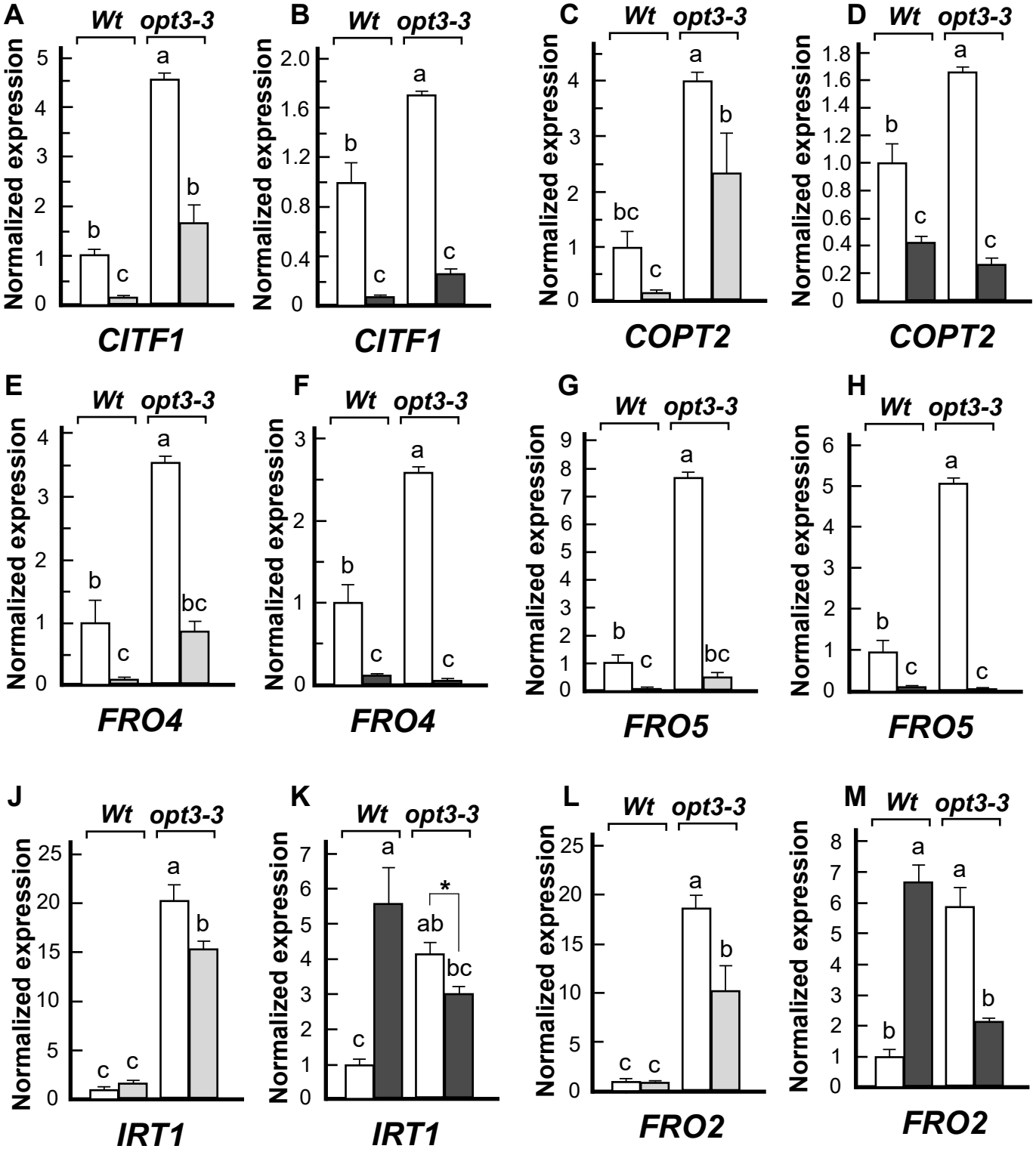

Figure 8. Copper supplementation partially rescues the molecular symptoms of copper deficiency in the *opt3* mutant.

Plants were grown hydroponically under control conditions (**white bars**) until the late-vegetative stage before a subset of plants was transferred to a fresh medium with higher copper concentrations (250 nM $CuSO_4$, **light grey bars** in **A, B, E, F, J, K** or 500 nM $CuSO_4$, **dark grey bars** in **C, D, G, H, L, M**). Plants were grown for another week prior to tissue collection and RT-qPCR analysis. The transcript abundance of indicated genes was normalized to the wild type grown under control conditions. Data show mean values ± S.E. Levels not connected by the same letter are statistically different (Tukey HSD, JMP Pro 14 software package, n = 3 independent experiments with roots pooled from 3 plants per each experiment).

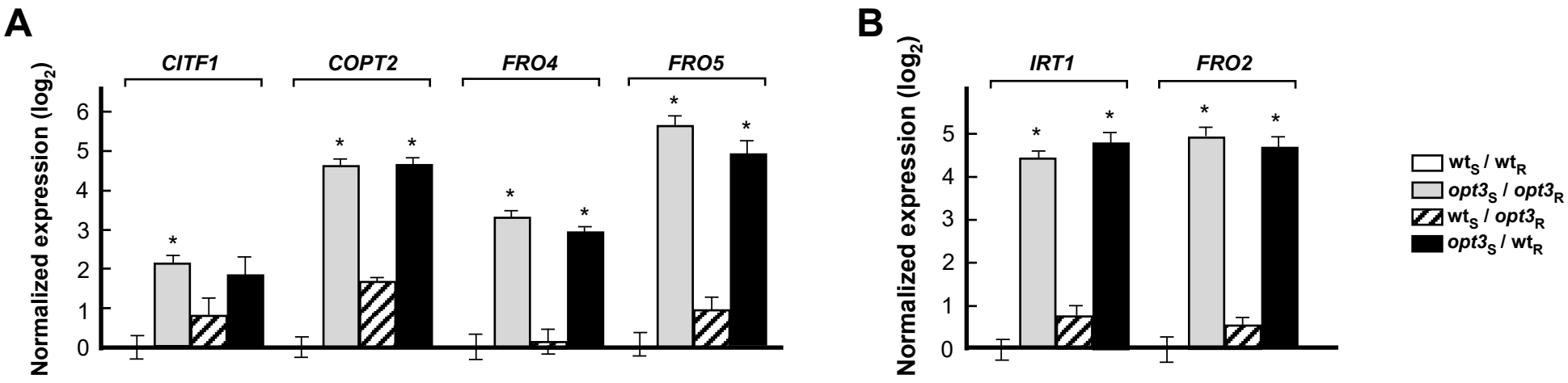

Figure 9. The expression of copper deficiency markers is controlled by the OPT3 function in the shoot.

The transcript abundance of copper- (**A**) and iron-deficiency (**B**) markers in roots of grafted plants. Wild type and the *opt3* mutant were used for reciprocal grafting. **Wt*S*/Wt*R*,** wild type scion grafted to wild type rootstock (control); ***opt3S/opt3R***, *opt3* scion grafted to *opt3* rootstock; **Wt*S*/opt3*R***, wild type scion grafted to *opt3* rootstock; ***opt3S/WtR***, *opt3* scion grafted to wild type rootstock. Shown values represent means ± S.E. Asterisks (*) indicate statistically significant values of the expression level is > 2 or <0.5 compared to control grafts ($p < 0.05$, based on CFX Manager 3.1 (BIO-RAD). Shown data are representative of three independent experiments.

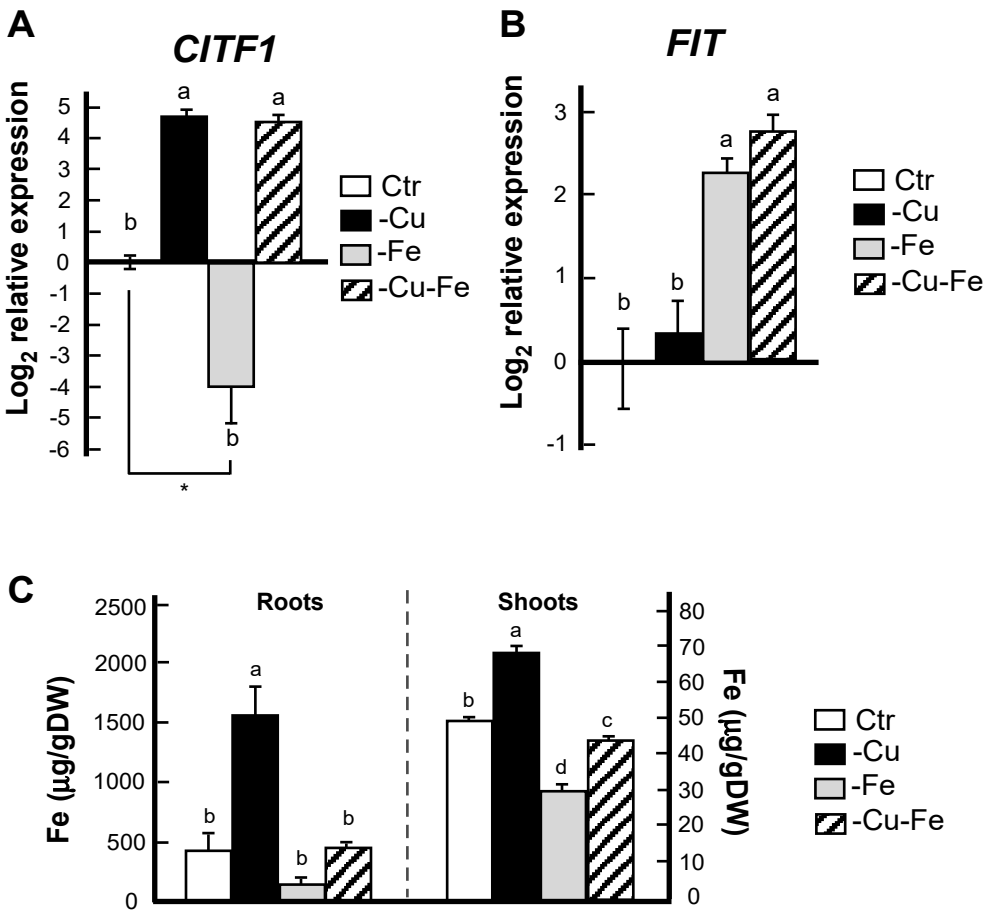

Figure 10. Copper and iron deficiency applied simultaneously increase the expression of *CITF1* and *FIT*, iron uptake and delivery to shoots.

The transcript abundance of *CITF1* **(A)**, *FIT* **(B)** and iron concentration in roots **(C)** were analyzed in plants grown under control conditions (**Ctr**) or without cooper but with iron **(-Cu)** for four weeks prior to tissue collection. To achieve iron deficiency, plants were grown under control conditions for three weeks, transferred to a solution without iron and grown for one additional week **(-Fe)**. For the simultaneous iron and copper deficiency treatment, plants were grown without copper but with iron for three weeks and then transferred to a fresh hydroponic medium lacking both copper and iron. Tissues were collected and analysed after an additional week of growth **(-Cu -Fe)**. Mean values ± S.E are shown. Levels not connected by the same letter are statistically different (Tukey HSD, JMP Pro 14 software package, n = 3 independent experiments with roots pooled from 3 plants per each experiment).

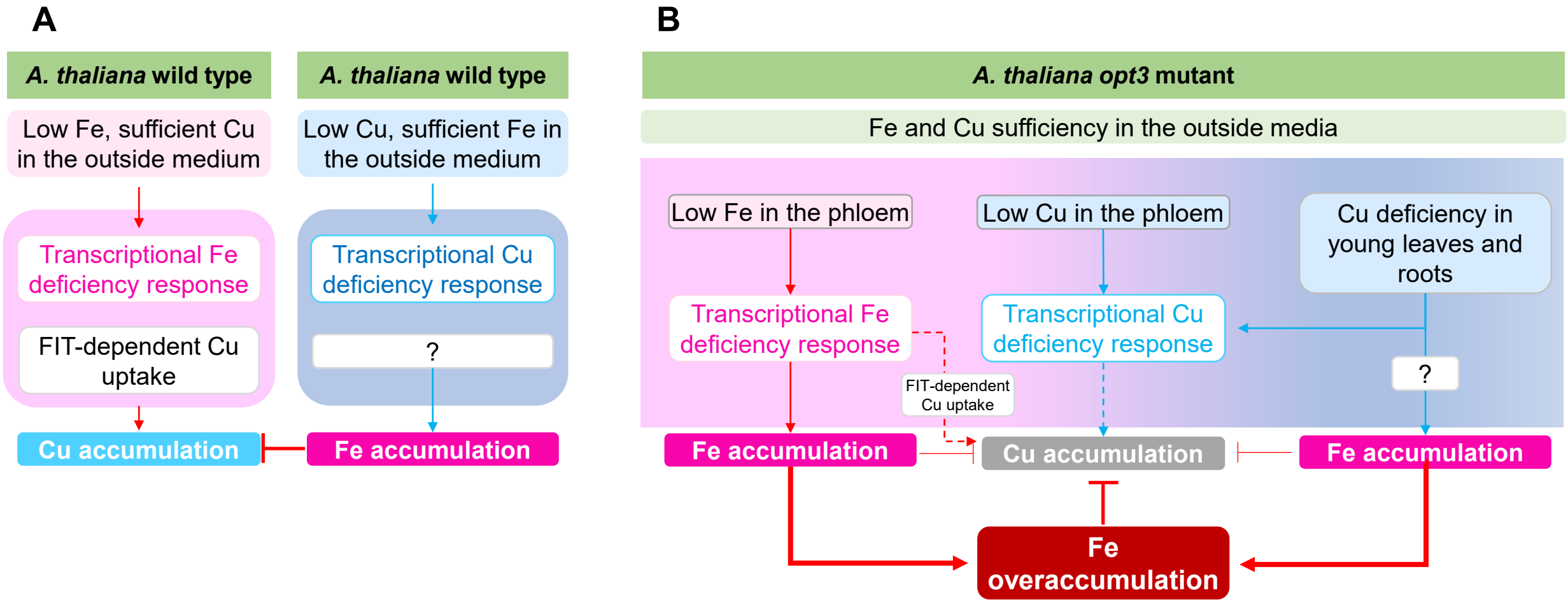

Figure 11. Altered Fe-Cu crosstalk in the *opt3* mutant contributes to iron over-accumulation. As illustrated in (**A**), iron deficiency in the outside medium causes copper accumulation in roots and leaves of *A. thaliana* wild type while copper deficiency in the outside medium results in iron accumulation (Bernal et al., 2012; Waters et al., 2012; Waters and Armbrust, 2013; Waters et al., 2014). By contrast, high iron status can repress copper accumulation in *A. thaliana* (Waters and Armbrust, 2013)**.** This has been also documented in animal species (Klevay, 2001; Ha et al., 2016). In the *opt3* mutant (**B**) the scenario is different in that, although both iron and copper are available in the outside medium, the *opt3* mutant experiences simultaneous iron and copper deficiency in the phloem (**Low Fe in the phloem; Low Cu in the Phloem**, respectively). Low iron accumulation in the phloem stimulates transcriptional iron deficiency response and iron accumulation since iron is available in the outside medium. Copper deficiency in the phloem, roots and leaves also lead to iron accumulation and transcriptional copper deficiency response. Increased iron accumulation from both pathways, in turn, decreases copper uptake further altering Fe-Cu crosstalk.

Parsed Citations

Agyeman-Budu DN, Choudhury S, Coulthard I, Gordon R, Hallin E, Woll AR (2016) Germanium Collimating micro-Channel Arrays For High Resolution, High Energy Confocal X-ray Fluorescence Microscopy. Icxom23: International Conference on X-Ray Optics and Microanalysis 1764
Google Scholar: Author Only Title Only Author and Title

Alexander SPH, Kelly E, Mathie A, Peters JA, Veale EL, Armstrong JF, Faccenda E, Harding SD, Pawson AJ, Sharman JL, et al. (2019) THE CONCISE GUIDE TO PHARMACOLOGY 2019/20: Transporters. British Journal of Pharmacology 176: S397-S493
Google Scholar: Author Only Title Only Author and Title

Araki R, Mermod M, Yamasaki H, Kamiya T, Fujiwara T, Shikanai T (2018) SPL7 locally regulates copper-homeostasis-related genes in Arabidopsis. J Plant Physiol 224-225: 137-143
Google Scholar: Author Only Title Only Author and Title

Bashir K, Ishimaru Y, Itai RN, Senoura T, Takahashi M, An G, Oikawa T, Ueda M, Sato A, Uozumi N, et al. (2015) Iron deficiency regulated OsOPT7 is essential for iron homeostasis in rice. Plant Molecular Biology 88: 165-176
Google Scholar: Author Only Title Only Author and Title

Baxter IR, Vitek O, Lahner B, Muthukumar B, Borghi M, Morrissey J, Guerinot ML, Salt DE (2008) The leaf ionome as a multivariable system to detect a plant's physiological status. Proceedings of the National Academy of Sciences 105: 12081-12086
Google Scholar: Author Only Title Only Author and Title

Benjamini Y, Hochberg Y (1995) Controlling the False Discovery Rate: A Practical and Powerful Approach to Multiple Testing. Journal of the Royal Statistical Society. Series B (Methodological) 57: 289-300
Google Scholar: Author Only Title Only Author and Title

Bernal M, Casero D, Singh V, Wilson GT, Grande A, Yang H, Dodani SC, Pellegrini M, Huijser P, Connolly EL, et al. (2012) Transcriptome sequencing identifies SPL7-regulated copper acquisition genes FRO4/FRO5 and the copper dependence of iron homeostasis in Arabidopsis. Plant Cell 24: 738-761
Google Scholar: Author Only Title Only Author and Title

Bernal M, Casero D, Singh V, Wilson GT, Grande A, Yang H, Dodani SC, Pellegrini M, Huijser P, Connolly EL, et al. (2012) Transcriptome Sequencing Identifies SPL7-Regulated Copper Acquisition Genes FRO4/FRO5 and the Copper Dependence of Iron Homeostasis in Arabidopsis. The Plant Cell Online 24: 738-761
Google Scholar: Author Only Title Only Author and Title

Bernal M, Casero D, Singh V, Wilson GT, Grande A, Yang H, Dodani SC, Pellegrini M, Huijser P, Connolly EL, et al. (2012) Transcriptome Sequencing Identifies SPL7 -Regulated Copper Acquisition Genes FRO4 FRO5 and the Copper Dependence of Iron Homeostasis in Arabidopsis The Plant Cell 24: 738-761
Google Scholar: Author Only Title Only Author and Title

BOGS J, BOURBOULOUX A, CAGNAC O, WACHTER A, RAUSCH T, DELROT S (2003) Functional characterization and expression analysis of a glutathione transporter, BjGT1, from Brassica juncea: evidence for regulation by heavy metal exposure. Plant, Cell & Environment 26: 1703-1711
Google Scholar: Author Only Title Only Author and Title

Broadley M, Brown P, Cakmak I, Rengel Z, Zhao F (2012) Chapter 7 - Function of Nutrients: Micronutrients A2 - Marschner, Petra. In Marschner's Mineral Nutrition of Higher Plants (Third Edition). Academic Press, San Diego, pp 191-248
Google Scholar: Author Only Title Only Author and Title

Burkhead JL, Gogolin Reynolds KA, Abdel-Ghany SE, Cohu CM, Pilon M (2009) Copper homeostasis. New Phytologist 182: 799-816
Google Scholar: Author Only Title Only Author and Title

Cagnac O, Bourbouloux A, Chakrabarty D, Zhang MY, Delrot S (2004) AtOPT6 transports glutathione derivatives and is induced by primisulfuron. Plant Physiology 135: 1378-1387
Google Scholar: Author Only Title Only Author and Title

Chang CJ (2015) Searching for harmony in transition-metal signaling. Nat Chem Biol 11: 744-747
Google Scholar: Author Only Title Only Author and Title

Chen C, Galon Y, Rahmati Ishka M, Malihi S, Shimanovsky V, Twito S, Rath A, Vatamaniuk OK, Miller G (2020) ASCORBATE PEROXIDASE6 delays the onset of age-dependent leaf senescence. Plant Physiology
Google Scholar: Author Only Title Only Author and Title

Colangelo EP, Guerinot ML (2004) The essential basic helix-loop-helix protein FIT1 is required for the iron deficiency response. Plant Cell 16: 3400-3412
Google Scholar: Author Only Title Only Author and Title

Cui Y, Chen CL, Cui M, Zhou WJ, Wu HL, Ling HQ (2018) Four IVa bHLH Transcription Factors Are Novel Interactors of FIT and Mediate JA Inhibition of Iron Uptake in Arabidopsis. Mol Plant 11: 1166-1183
Google Scholar: Author Only Title Only Author and Title

Dancis A, Haile D, Yuan DS, Klausner RD (1994) The Saccharomyces cerevisiae copper transport protein (Ctr1p). Biochemical characterization, regulation by copper, and physiologic role in copper uptake. J Biol Chem 269: 25660-25667
Google Scholar: Author Only Title Only Author and Title

Epstein E, Bloom A (2005) Mineral nutrition of plants: principles and perspectives, 2nd eds. Sunderland, Mass Sinaur: 292-305
Google Scholar: Author Only Title Only Author and Title

Gao F, Robe K, Bettembourg M, Navarro N, Rofidal V, Santoni V, Gaymard F, Vignols F, Roschzttardtz H, Izquierdo E, et al. (2020) The Transcription Factor bHLH121 Interacts with bHLH105 (ILR3) and Its Closest Homologs to Regulate Iron Homeostasis in Arabidopsis. Plant Cell 32: 508-524
Google Scholar: Author Only Title Only Author and Title

Garcia MJ, Romera FJ, Stacey MG, Stacey G, Villar E, Alcantara E, Perez-Vicente R (2013) Shoot to root communication is necessary to control the expression of iron-acquisition genes in Strategy I plants. Planta 237: 65-75
Google Scholar: Author Only Title Only Author and Title

Gayomba SR, Jung H-i, Yan J, Danku J, Rutzke MA, Bernal M, Kramer U, Kochian LV, Salt DE, Vatamaniuk OK (2013) The CTR/COPT-dependent copper uptake and SPL7-dependent copper deficiency responses are required for basal cadmium tolerance in A. thaliana. Metallomics 5: 1262-1275
Google Scholar: Author Only Title Only Author and Title

Gayomba SR, Jung HI, Yan J, Danku J, Rutzke MA, Bernal M, Kramer U, Kochian LV, Salt DE, Vatamaniuk OK (2013) The CTR/COPT-dependent copper uptake and SPL7-dependent copper deficiency responses are required for basal cadmium tolerance in A. thaliana. Metallomics 5: 1262-1275
Google Scholar: Author Only Title Only Author and Title

Gayomba SR, Zhai Z, Jung HI, Vatamaniuk OK (2015) Local and systemic signaling of iron status and its interactions with homeostasis of other essential elements. Front Plant Sci 6: 716
Google Scholar: Author Only Title Only Author and Title

Grillet L, Lan P, Li W, Mokkapati G, Schmidt W (2018) IRON MAN is a ubiquitous family of peptides that control iron transport in plants. Nat Plants 4: 953-963
Google Scholar: Author Only Title Only Author and Title

Ha JH, Doguer C, Wang X, Flores SR, Collins JF (2016) High-Iron Consumption Impairs Growth and Causes Copper-Deficiency Anemia in Weanling Sprague-Dawley Rats. PLoS One 11: e0161033
Google Scholar: Author Only Title Only Author and Title

Hirayama T, Lei GJ, Yamaji N, Nakagawa N, Ma JF (2018) The Putative Peptide Gene FEP1 Regulates Iron Deficiency Response in Arabidopsis. Plant Cell Physiol 59: 1739-1752
Google Scholar: Author Only Title Only Author and Title

Jain A, Wilson G, Connolly E (2014) The diverse roles of FRO family metalloreductases in iron and copper homeostasis. Frontiers in Plant Science 5
Google Scholar: Author Only Title Only Author and Title

Jeong J, Merkovich A, Clyne M, Connolly EL (2017) Directing iron transport in dicots: regulation of iron acquisition and translocation. Curr Opin Plant Biol 39: 106-113
Google Scholar: Author Only Title Only Author and Title

Jiang A, Guo Z, Pan J, Zhuang Y, Zuo D, Hao C, Gao Z, Xin P, Chu J, Zhong S, et al. (2020) The PIF1-MIR408-Plantacyanin Repression Cascade Regulates Light Dependent Seed Germination. bioRxiv: 2020.2007.2020.212340
Google Scholar: Author Only Title Only Author and Title

Joung J-G, Corbett AM, Fellman SM, Tieman DM, Klee HJ, Giovannoni JJ, Fei Z (2009) Plant MetGenMAP: An Integrative Analysis System for Plant Systems Biology. Plant Physiology 151: 1758-1768
Google Scholar: Author Only Title Only Author and Title

Jung H-i, Gayomba SR, Rutzke MA, Craft E, Kochian LV, Vatamaniuk OK (2012) COPT6 is a plasma membrane transporter that functions in copper homeostasis in Arabidopsis and is a novel target of SQUAMOSA promoter-binding protein-like 7. The Journal of biological chemistry 287: 33252-33267
Google Scholar: Author Only Title Only Author and Title

Jung HI, Gayomba SR, Rutzke MA, Craft E, Kochian LV, Vatamaniuk OK (2012) COPT6 is a plasma membrane transporter that functions in copper homeostasis in Arabidopsis and is a novel target of SQUAMOSA promoter-binding protein-like 7. J Biol Chem 287: 33252-33267
Google Scholar: Author Only Title Only Author and Title

Kastoori Ramamurthy R, Xiang Q, Hsieh EJ, Liu K, Zhang C, Waters BM (2018) New aspects of iron-copper crosstalk uncovered by transcriptomic characterization of Col-0 and the copper uptake mutant spl7 in Arabidopsis thaliana. Metallomics 10: 1824-1840
Google Scholar: Author Only Title Only Author and Title

Khan MA, Castro-Guerrero NA, McInturf SA, Nguyen NT, Dame AN, Wang J, Bindbeutel RK, Joshi T, Jurisson SS, Nusinow DA, et al.

(2018) Changes in iron availability in Arabidopsis are rapidly sensed in the leaf vasculature and impaired sensing leads to opposite transcriptional programs in leaves and roots. Plant, Cell & Environment 41: 2263-2276
Google Scholar: Author Only Title Only Author and Title

Khan MA, Castro-Guerrero NA, McInturf SA, Nguyen NT, Dame AN, Wang J, Bindbeutel RK, Joshi T, Jurisson SS, Nusinow DA, et al. (2018) Changes in iron availability in Arabidopsis are rapidly sensed in the leaf vasculature and impaired sensing leads to opposite transcriptional programs in leaves and roots. Plant Cell Environ 41: 2263-2276
Google Scholar: Author Only Title Only Author and Title

Kim SA, LaCroix IS, Gerber SA, Guerinot ML (2019) The iron deficiency response in Arabidopsis thaliana requires the phosphorylated transcription factor URI. Proceedings of the National Academy of Sciences 116: 24933-24942
Google Scholar: Author Only Title Only Author and Title

Kim SA, Punshon T, Lanzirotti A, Li L, Alonso JM, Ecker JR, Kaplan J, Guerinot ML (2006) Localization of Iron in *Arabidopsis* Seed Requires the Vacuolar Membrane Transporter VIT1. Science 314: 1295-1298
Google Scholar: Author Only Title Only Author and Title

Klevay LM (2001) Iron overload can induce mild copper deficiency. J Trace Elem Med Biol 14: 237-240
Google Scholar: Author Only Title Only Author and Title

Kobayashi T (2019) Understanding the Complexity of Iron Sensing and Signaling Cascades in Plants. Plant Cell Physiol 60: 1440-1446
Google Scholar: Author Only Title Only Author and Title

Kroh GE, Pilon M (2020) Micronutrient homeostasis and chloroplast iron protein expression is largely maintained in a chloroplast copper transporter mutant. Funct Plant Biol 47: 1041-1052
Google Scholar: Author Only Title Only Author and Title

Kumar RK, Chu H-H, Abundis C, Vasques K, Rodriguez DC, Chia J-C, Huang R, Vatamaniuk OK, Walker EL (2017) Iron-Nicotianamine Transporters Are Required for Proper Long Distance Iron Signaling Plant Physiology 175: 1254-1268
Google Scholar: Author Only Title Only Author and Title

Kumar RK, Chu HH, Abundis C, Vasques K, Rodriguez DC, Chia JC, Huang R, Vatamaniuk OK, Walker EL (2017) Iron-Nicotianamine Transporters Are Required for Proper Long Distance Iron Signaling. Plant Physiol 175: 1254-1268
Google Scholar: Author Only Title Only Author and Title

Kurt F (2021) An Insight into Oligopeptide Transporter 3 (OPT3) Family Proteins. Protein and Peptide Letters 28: 43-54
Google Scholar: Author Only Title Only Author and Title

Langmead B, Trapnell C, Pop M, Salzberg SL (2009) Ultrafast and memory-efficient alignment of short DNA sequences to the human genome. Genome Biology 10: R25
Google Scholar: Author Only Title Only Author and Title

Li WF, Lan P (2017) The Understanding of the Plant Iron Deficiency Responses in Strategy I Plants and the Role of Ethylene in This Process by Omic Approaches. Frontiers in Plant Science 8
Google Scholar: Author Only Title Only Author and Title

Love MI, Huber W, Anders S (2014) Moderated estimation of fold change and dispersion for RNA-seq data with DESeq2. Genome Biology 15: 550
Google Scholar: Author Only Title Only Author and Title

Lubkowitz M (2011) The Oligopeptide Transporters: A Small Gene Family with a Diverse Group of Substrates and Functions? Mol Plant 4: 407-415
Google Scholar: Author Only Title Only Author and Title

Maas FM, van de Wetering DA, van Beusichem ML, Bienfait HF (1988) Characterization of phloem iron and its possible role in the regulation of Fe-efficiency reactions. Plant Physiol 87: 167-171
Google Scholar: Author Only Title Only Author and Title

Mai HJ, Lindermayr C, von Toerne C, Fink-Straube C, Durner J, Bauer P (2015) Iron and FER-LIKE IRON DEFICIENCY-INDUCED TRANSCRIPTION FACTOR-dependent regulation of proteins and genes in Arabidopsis thaliana roots. Proteomics 15: 3030-3047
Google Scholar: Author Only Title Only Author and Title

Malzer W, Kanngießer B (2005) A Model for the Confocal Volume of 3D Micro X-ray Fluorescence Spectrometer. Spectrochimica Acta Part B: Atomic Spectroscopy 60: 1334-1341
Google Scholar: Author Only Title Only Author and Title

Mantouvalou I, Malzer W, Kanngießer B (2012) Quantification for 3D micro X-ray fluorescence. Spectrochimica Acta Part B: Atomic Spectroscopy 77: 9-18
Google Scholar: Author Only Title Only Author and Title

Mantouvalou I, Malzer W, Kanngiesser B (2012) Quantification for 3D micro X-ray fluorescence. Spectrochimica Acta Part B-Atomic Spectroscopy 77: 9-18
Google Scholar: Author Only Title Only Author and Title

Mendoza-Cózatl DG, Xie Q, Akmakjian GZ, Jobe TO, Patel A, Stacey MG, Song L, Demoin DW, Jurisson SS, Stacey G, et al. (2014) OPT3 is a component of the iron-signaling network between leaves and roots and misregulation of OPT3 leads to an over-accumulation of cadmium in seeds. Mol Plant 7: 1455-1469
Google Scholar: Author Only Title Only Author and Title

Mukherjee I, Campbell NH, Ash JS, Connolly EL (2006) Expression profiling of the Arabidopsis ferric chelate reductase (FRO) gene family reveals differential regulation by iron and copper. Planta 223: 1178-1190
Google Scholar: Author Only Title Only Author and Title

Newville M (2013) Larch: An Analysis Package for XAFS and Related Spectroscopies. J. Phys.: Conf. Ser. 430
Google Scholar: Author Only Title Only Author and Title

Osawa H, Stacey G, Gassmann W (2006) ScOPT1 and AtOPT4 function as proton-coupled oligopeptide transporters with broad but distinct substrate specificities. Biochemical Journal 393: 267-275
Google Scholar: Author Only Title Only Author and Title

Pottier M, Dumont J, Masclaux-Daubresse C, Thomine S (2019) Autophagy is essential for optimal translocation of iron to seeds in Arabidopsis. Journal of experimental botany 70: 859-869
Google Scholar: Author Only Title Only Author and Title

Quast C, Pruesse E, Yilmaz P, Gerken J, Schweer T, Yarza P, Peplies J, Glöckner FO (2013) The SILVA ribosomal RNA gene database project: improved data processing and web-based tools. Nucleic Acids Research 41: 7
Google Scholar: Author Only Title Only Author and Title

Rahmati Ishka M, Vatamaniuk OK (2020) Copper deficiency alters shoot architecture and reduces fertility of both gynoecium and androecium in Arabidopsis thaliana. BioRxiv
Google Scholar: Author Only Title Only Author and Title

Rahmati Ishka M, Vatamaniuk OK (2020) Copper deficiency alters shoot architecture and reduces fertility of both gynoecium and androecium in Arabidopsis thaliana. Plant Direct 4: e00288
Google Scholar: Author Only Title Only Author and Title

Rai S, Singh PK, Mankotia S, Swain J, Satbhai SB (2021) Iron homeostasis in plants and its crosstalk with copper, zinc, and manganese. Plant Stress 1: 100008
Google Scholar: Author Only Title Only Author and Title

Ravet K, Danford FL, Dihle A, Pittarello M, Pilon M (2011) Spatiotemporal Analysis of Copper Homeostasis in Populus trichocarpa Reveals an Integrated Molecular Remodeling for a Preferential Allocation of Copper to Plastocyanin in the Chloroplasts of Developing Leaves. Plant Physiology 157: 1300-1312
Google Scholar: Author Only Title Only Author and Title

Ravet K, Pilon M (2013) Copper and Iron Homeostasis in Plants: The Challenges of Oxidative Stress. Antioxidants & Redox Signaling 19: 23
Google Scholar: Author Only Title Only Author and Title

Rees EM, Lee J, Thiele DJ (2004) Mobilization of Intracellular Copper Stores by the Ctr2 Vacuolar Copper Transporter. Journal of Biological Chemistry 279: 54221-54229
Google Scholar: Author Only Title Only Author and Title

Rodríguez FI, Esch JJ, Hall AE, Binder BM, Schaller GE, Bleecker AB (1999) A Copper Cofactor for the Ethylene Receptor ETR1 from Arabidopsis. Science 283: 996-998
Google Scholar: Author Only Title Only Author and Title

Schott-Verdugo S, Müller L, Classen E, Gohlke H, Groth G (2019) Structural Model of the ETR1 Ethylene Receptor Transmembrane Sensor Domain. Scientific Reports 9: 8869
Google Scholar: Author Only Title Only Author and Title

Schwarz B, Bauer P (2020) FIT, a regulatory hub for iron deficiency and stress signaling in roots, and FIT-dependent and -independent gene signatures. J Exp Bot 71: 1694-1705
Google Scholar: Author Only Title Only Author and Title

Shahbaz M, Ravet K, Peers G, Pilon M (2015) Prioritization of copper for the use in photosynthetic electron transport in developing leaves of hybrid poplar. Frontiers in Plant Science 6
Google Scholar: Author Only Title Only Author and Title

Sheng H, Jiang Y, Ishka MR, Chia J-C, Dokuchayeva T, Kavulych Y, Zavodna T-O, Mendoza PN, Huang R, Smieshka LM, et al. (2021) YSL3-mediated copper distribution is required for fertility, grain yield, and size in Brachypodium. Plant Physiology: 2019.2012.2012.874396
Google Scholar: Author Only Title Only Author and Title

Sheng H, Jiang Y, Ishka MR, Chia JC, Dokuchayeva T, Kavulych Y, Zavodna TO, Mendoza PN, Huang R, Smieshka LM, et al. (2021) YSL3-mediated copper distribution is required for fertility, seed size and protein accumulation in Brachypodium. Plant Physiol 186: 655-676

Google Scholar: Author Only Title Only Author and Title

Solé VA, Papillon E, Cotte M, Walter P, Susini J (2007) A multiplatform code for the analysis of energy-dispersive X-ray fluorescence spectra. Spectrochimica Acta Part B: Atomic Spectroscopy 62: 63-68
Google Scholar: Author Only Title Only Author and Title

Spielmann J, Vert G (2020) The many facets of protein ubiquitination and degradation in plant root iron-deficiency responses. Journal of Experimental Botany 72: 2071-2082
Google Scholar: Author Only Title Only Author and Title

Stacey MG, Koh S, Becker J, Stacey G (2002) AtOPT3, a Member of the Oligopeptide Transporter Family, Is Essential for Embryo Development in Arabidopsis. The Plant Cell 14: 2799-2811
Google Scholar: Author Only Title Only Author and Title

Stacey MG, Patel A, McClain WE, Mathieu M, Remley M, Rogers EE, Gassmann W, Blevins DG, Stacey G (2008) The Arabidopsis AtOPT3 Protein Functions in Metal Homeostasis and Movement of Iron to Developing Seeds. Plant Physiology 146: 589-601
Google Scholar: Author Only Title Only Author and Title

Trapnell C, Pachter L, Salzberg SL (2009) TopHat: discovering splice junctions with RNA-Seq. Bioinformatics 25: 7
Google Scholar: Author Only Title Only Author and Title

Tsang T, Posimo JM, Gudiel AA, Cicchini M, Feldser DM, Brady DC (2020) Copper is an essential regulator of the autophagic kinases ULK1/2 to drive lung adenocarcinoma. Nature cell biology 22: 412-424
Google Scholar: Author Only Title Only Author and Title

Turski ML, Brady DC, Kim HJ, Kim BE, Nose Y, Counter CM, Winge DR, Thiele DJ (2012) A novel role for copper in Ras/mitogen-activated protein kinase signaling. Mol Cell Biol 32: 1284-1295
Google Scholar: Author Only Title Only Author and Title

Turski ML, Thiele DJ (2009) New roles for copper metabolism in cell proliferation, signaling, and disease. J Biol Chem 284: 717-721
Google Scholar: Author Only Title Only Author and Title

Waters BM, Armbrust LC (2013) Optimal copper supply is required for normal plant iron deficiency responses. Plant Signal Behav 8: e26611
Google Scholar: Author Only Title Only Author and Title

Waters BM, McInturf SA, Amundsen K (2014) Transcriptomic and physiological characterization of the fefe mutant of melon (Cucumis melo) reveals new aspects of iron-copper crosstalk. New Phytol 203: 1128-1145
Google Scholar: Author Only Title Only Author and Title

Waters BM, McInturf SA, Stein RJ (2012) Rosette iron deficiency transcript and microRNA profiling reveals links between copper and iron homeostasis in Arabidopsis thaliana. J Exp Bot 63: 5903-5918
Google Scholar: Author Only Title Only Author and Title

Wongkaew A, Asayama K, Kitaiwa T, Nakamura SI, Kojima K, Stacey G, Sekimoto H, Yokoyama T, Ohkama-Ohtsu N (2018) AtOPT6 Protein Functions in Long-Distance Transport of Glutathione in Arabidopsis thaliana. Plant and Cell Physiology 59: 1443-1451
Google Scholar: Author Only Title Only Author and Title

Wu Y, Zhang D, Chu Jee Y, Boyle P, Wang Y, Brindle Ian D, De Luca V, Després C (2012) The Arabidopsis NPR1 Protein Is a Receptor for the Plant Defense Hormone Salicylic Acid. Cell Reports 1: 639-647
Google Scholar: Author Only Title Only Author and Title

Yamasaki H, Hayashi M, Fukazawa M, Kobayashi Y, Shikanai T (2009) SQUAMOSA Promoter Binding Protein-Like7 Is a Central Regulator for Copper Homeostasis in Arabidopsis. Plant Cell 21: 347-361
Google Scholar: Author Only Title Only Author and Title

Yan J, Chia J-C, Sheng H, Jung H-i, Zavodna T-O, Zhang L, Huang R, Jiao C, Craft EJ, Fei Z, et al. (2017) Arabidopsis Pollen Fertility Requires the Transcription Factors CITF1 and SPL7 That Regulate Copper Delivery to Anthers and Jasmonic Acid Synthesis. The Plant Cell 29: 3012-3029
Google Scholar: Author Only Title Only Author and Title

Zhai Z, Gayomba SR, Jung H-I, Vimalakumari NK, Piñeros M, Craft E, Rutzke MA, Danku J, Lahner B, Punshon T, et al. (2014) OPT3 Is a Phloem-Specific Iron Transporter That Is Essential for Systemic Iron Signaling and Redistribution of Iron and Cadmium in Arabidopsis. The Plant cell 26: 2249-2264
Google Scholar: Author Only Title Only Author and Title

Zhai Z, Gayomba SR, Jung H-i, Vimalakumari NK, Piñeros M, Craft E, Rutzke MA, Danku J, Lahner B, Punshon T, et al. (2014) OPT3 is a phloem-specific iron transporter that is essential for systemic iron signaling and redistribution of iron and cadmium in Arabidopsis. Plant Cell 26: 2249-2264
Google Scholar: Author Only Title Only Author and Title

Zhang Z, Xie Q, Jobe TO, Kau AR, Wang C, Li Y, Qiu B, Wang Q, Mendoza-Cózatl DG, Schroeder JI (2016) Identification of AtOPT4 as a Plant Glutathione Transporter. Mol Plant 9: 481-484
Google Scholar: Author Only Title Only Author and Title

Zhong S, Joung J-G, Zheng Y, Chen Y-r, Liu B, Shao Y, Xiang JZ, Fei Z, Giovannoni JJ (2011) High-Throughput Illumina Strand-Specific RNA Sequencing Library Preparation. Cold Spring Harbor Protocols 2011: pdb.prot5652

Google Scholar: Author Only Title Only Author and Title